Cell Tissue Res (2008) 333:17–27
DOI 10.1007/s00441-008-0618-4

REGULAR ARTICLE

Hepatoblast-like cells enriched from mouse embryonic stem cells in medium without glucose, pyruvate, arginine, and tyrosine

Minoru Tomizawa · Yoshiro Toyama · Chizuru Ito · Kiyotaka Toshimori · Katsuro Iwase · Masaki Takiguchi · Hiromitsu Saisho · Osamu Yokosuka

Received: 15 November 2007 / Accepted: 31 March 2008 / Published online: 14 May 2008

Abstract In order to enrich hepatocytes differentiated from embryonic stem cells, we developed a novel medium. Since only hepatocytes have the activity of ornithine transcarbamylase, phenylalanine hydroxylase, galactokinase, and glycerol kinase, we expected that hepatocytes would be enriched in a medium without arginine, tyrosine, glucose, and pyruvate, but supplemented with ornithine, phenylanaline, galactose, and glycerol (hepatocyte-selection medium, HSM). Embryoid bodies were transferred onto dishes coated with gelatin in HSM after 4 days of culture. At 18 days after embryoid body formation, a single type of polygonal cell survived with an enlarged intercellular space and micorvilli. These cells were positive for indocyanine green uptake and for mRNAs of albumin, transthyretin, and α-feto protein, but negative for mRNAs of tyrosine aminotransferase, α1-antitrypsin, glucose-6-phosphatase, and phosphoenol pyruvate carboxykinase. Since cells in HSM were positive for cytokeratin (CK) 8 and CK18 (hepatocyte markers) and for CK19 (a marker of bile duct epithelial cells), we concluded that they were hepatoblasts. They showed weaker expression of CCAAT/enhancer-binding protein (C/EBP)α than fetal liver (18.5 days of gestation) and expression of C/EBPβ at a similar level to that of fetal liver. These data support our conclusion that HSM allows the selection of hepatoblast-like cells.

Keywords Hepatocyte · Differentiation · Ornithine carbamoyltransferase · Galactokinase · Indocyanine green · Mouse (EB5 cell line)

This work was supported by the Tsuchiya Foundation, the Ichiro Kanehara Foundation, and a Research Grant-in-Aid for Scientific Research from Japan Society for the Promotion of Science.

M. Tomizawa (✉) · H. Saisho · O. Yokosuka
Department of Medicine and Clinical Oncology,
Graduate School of Medicine, Chiba University,
1–8–1 Inohana, Chuo-ku,
Chiba City, Chiba 260–8670, Japan
e-mail: nihminor-cib@umin.ac.jp

Y. Toyama · C. Ito · K. Toshimori
Department of Anatomy and Developmental Biology,
Graduate School of Medicine, Chiba University,
Chiba City, Chiba, Japan

K. Iwase · M. Takiguchi
Department of Biochemistry and Genetics,
Graduate School of Medicine, Chiba University,
Chiba City, Chiba, Japan

Introduction

Embryonic stem (ES) cells have shown promise for use in regenerative medicine because they produce various types of cells. If hepatocytes could be produced and enriched from ES cells, they might be transplantable to patients suffering from liver insufficiency or useful as a liver-assist device (Heo et al. 2006; Soto-Gutierrez et al. 2006). To date, various protocols have been reported regarding the differentiation protocol of ES cells to hepatocytes (Lavon and Benvenisty 2005): (1) ES cells can be differentiated to hepatocytes by withdrawal of leukemia inhibitory factor (LIF; Jones et al. 2002); (2) the differentiation of ES cells to hepatocytes is promoted by growth factors, such as hepatocyte growth factor, and extracellular matrix, such as type I collagen (Hamazaki et al. 2001); transcription factor, such as hepatocyte nuclear factor (HNF)-3β, has been

introduced to promote hepatocyte differentiaion from ES cells (Ishizaka et al. 2002). Although some of the cells are positive for genes specific to hepatocytes, others are not. If cells derived from ES cells are transplanted without enrichment of hepatocytes, teratoma will be formed (Teramoto et al. 2005). We therefore need to develop methods to purify hepatocytes differentiated from ES cells.

Hepatocytes differentiated from ES cells are enriched, for fluorescence-associated cell sorting, with green fluorescent protein driven by an albumin promoter as a marker of hepatocytes (Heo et al. 2006). Ethical problems may arise in the application of this method for humans in a clinical setting, since this requires the introduction of foreign genes into humans. Hepatocytes can be successfully enriched by Percoll gradient centrifugation followed by magnetic cell sorting (Kumashiro et al. 2005). One problem of this method is that undifferentiated cells may contaminate hepatocytes. Another problem is that embryoid bodies are difficult to disaggregate, as they are tightly bound by their extracellular matrices. The development of a novel way to isolate hepactocytes from ES cells would therefore be desirable. Since hepatocytes produce metabolites necessary for cells to survive, e.g., via the urea cycle and gluconeogenesis, we expected that a medium lacking their products would enrich hepatocytes from cells differentiated from ES cells.

Endodermal patterning begins in a mouse embryo at the six-somite stage (Zaret 2002). Hepatic genes are induced in a segment of the definitive endoderm at 8.5 days of gestation. Expression of HNF-3β appears in endodermal cells, occupying the promoters of liver-specific genes (Bossard and Zaret 1998). Our method with medium lacking LIF (ESM) is a spontaneous differentiation protocol (Lavon and Benvenisty 2005). Hanging drop culture for 5 days has been used in previous reports, whereas we have employed 4 days in our protocol (Jones et al. 2002; Yamada et al. 2002). Similarly, 15% fetal calf serum (FCS) has been previously used, whereas we have chosen 10% FCS (Miyashita et al. 2002; Abe et al. 1996). Culture periods of 30 days for embryoid bodies on gelatin-coated dishes have been used formerly (Miyashita et al. 2002), but we have selected 14 days for our protocol. Sodium pyruvate has been included in our ESM, since withdrawal of LIF is used for differentiation. In our preliminary experiments, the decrease of cell number when deprived of sodium pyruvate prompted us to speculate that sodium pyruvate inhibited differentiation. Shorter culture in hanging drops and less FCS and sodium pyruvate might inhibit differentiation for the expression of albumin, although cells in ESM differentiate toward endoderm, as evidenced by HNF-3β and Delta like (Dlk)-1. We changed from ESM to hepatocyte-selection medium (HSM) at the same time of transfer of embryoid bodies to gelatin-coated dishes in order to enrich hepatoblast-like cells successfully, whereas cells in ESM remained at more immature state than those in HSM. We did not use any growth factors or extracellular matrix specific to hepatocyte differentiation. We proposed that the change of medium to HSM at 4 days of hanging drop culture would be suitable for ES cells to enrich hepatoblast-like cells. The endodermal cells proliferate and migrate into the septum transversum to form hepatic endoderm in which hepatoblasts appear. After 12 days of gestation, hepatoblasts start to differentiate into hepatocytes or biliary epithelial cells (Lavon and Benvenisty 2005). During hepatoctye differention, the expression of liver-specific transcription factors appears to up-regulate liver-specific genes. One example is that CCAAT-enhancer binding protein (C/EBP) α appears to promote the expression of ornithine transcarbamylase (OTC; Murakami et al. 1990). OTC, mainly expressed in hepatocytes, catalyzes the second step of the urea cycle to produce arginine.

Among all amino acids, withdrawal of arginine is tolerated the least by cultured cells in vitro (Wheatley et al. 2000). Arginine is produced via the urea cycle, which is exclusive to hepatocytes. Indeed, withdrawal of arginine led to the first medium for the purification of hepatocytes (Leffert and Paul 1972). Tyrosine is produced by hepatocytes. Interestingly, a subline of hepatoma cells is established in a medium deprived of serum, arginine, and tyrosine (Niwa et al. 1980). The cell line has the activity of OTC, which is involved in the urea cycle, and phenylalanine hydroxylase (PAH), which produces tyrosine. PAH is distributed in liver and kidney (McGee et al. 1972). Consequently, we might expect that hepatocytes can be enriched from ES cells in a medium without arginine and tyrosine.

Glucose is an important source of energy for the survival of cells. Withdrawal of glucose contributes to the enrichment of hepatocytes since they can produce it (Leffert and Paul 1972). Pyruvate, the final product of glycolysis, enters the citric acid cycle. When pyruvate plus glucose is withdrawn from the medium, all neural cells die (Matsumoto et al. 1994). Pyruvate is produced from phosphoenol pyruvate by pyruvate kinase (PK), expressed in liver, kidney, and red blood cells. Glycerol and galactose enter glycolysis via glycerol kinase (GK) and galactokinase, both of which are expressed in liver and kidney (Ai et al. 1995; Ohira et al. 2005). We therefore expected that hepatocytes would be specifically capable of surviving in the presence of galactose and glycerol and in the absence of either glucose or pyruvate (Phillips et al. 2002; Sumida et al. 2002).

Here, we have investigated whether we can enrich hepatocytes derived from ES cells in medium deprived of arginine, tyrosine, glucose, and pyruvate, and supplemented with ornithine, glycerol, and galactose. Insulin and dexamethasone have to be added, as they maintain primary cultured hepatocytes (Inoue et al. 1989).

Materials and methods

Cell culture, light microscopy, and cell counting

EB5, a cell line of mouse ES cells provided by Dr. H. Niwa (Center for Developmental Biology, Riken, Kobe, Japan), was maintained undifferentiated in dishes coated with gelatin (Sigma Aldrich Japan, Tokyo, Japan) without feeder cells in Glasgow minimum essential medium (GMEM; Sigma Aldrich Japan) supplemented with 10% FCS (Roche Diagnostics, Tokyo, Japan), 1× non-essential amino acids (Invitrogen Japan, Tokyo, Japan), sodium pyruvate (1 mM; Invitrogen), 2-mercaptoethanol (0.1 mM; Wako Pure Chemicals, Osaka, Japan), and LIF (1000 U/ml; Invitrogen; Niwa et al. 2002). To induce differentiation, dissociated ES cells were cultured in hanging drops at a density of 1,000 cells per 30 μl of the above media (based on GMEM) without LIF (ESM) to form embryoid bodies. After 4 days in hanging drop culture, the resulting embryoid bodies were plated onto plastic dishes (Iwaki-Asahi Techno Glass, Tokyo, Japan) coated with gelatin. To isolate hepatocytes differentiated from ES cells, the medium was changed into hepatocyte-selection medium (HSM) on the transfer of embryoid bodies onto dishes coated with gelatin. HSM was originally made from amino acid powders based on L15, deprived of arginine, tyrosine, glucose, or sodium pyruvate, but supplemented with galactose (900 mg/l; Wako), ornithine (1 mM; Wako), glycerol (5 mM; Wako), and proline (260 mM; Wako). Proline was added because of its requirement for DNA synthesis (Nakamura et al. 1984). Aspartic acid was withdrawn, it being one of the products of ornithine and a substrate of arginine. HSM was supplemented with insulin (10 μM; Sigma Aldrich), dexamethasone (10 μM; Wako), aprotinin (5,000 U/ml; Wako), and 2-mercaptoethanol (0.1 mM; Sigma Aldrich). FCS was added at a final concentration of 10% after dialysis against phosphate-buffered saline (PBS) to exclude amino acids and D(+)-glucose. Cells were observed microscopically with an IMT-2 (Olympus, Tokyo, Japan). Three embryoid bodies were transferred onto 6-well plates (Iwaki-Asahi) coated with gelatin and cultured in either ESM or HSM. Cells were washed with physiological saline, harvested with 0.05% trypsin-0.53 mM EDTA (Invitrogen), followed by cell counting by the trypan blue dye (Sigma Aldrich) exclusion test. The cell counting was repeated three times.

Electron microscopy

Grown colonies of hepatocyte-like cells in the culture dishes (Iwaki-Asahi) were selected under light microscopy, and the culture medium was discarded. Colonies remaining in the dish were fixed with 2.5% glutaraldehyde (TAAB, Aldermaston, UK) in HEPES buffer (pH 7.4) for 2 h at room temperature. After being washed gently with the HEPES buffer, the cells were postfixed with 1% osmium tetroxide for 15 min. Then, the cells were dehydrated in a graded ethanol series, immersed in a mixture of ethanol and Epon (1:1) for 15 min, and embedded in Epon.

After polymerization, the Epon disc containing the cell colonies was removed from the culture dish. Colonies of cells for observation were selected under a binocular or inverted light microscope. Sections were cut parallel to the disc surface. Semi-thin sections were stained with toluidine blue for light microscopy, and ultra-thin sections were stained with uranyl acetate and lead citrate for observation under an electron microscope (JEM 1200 Ex II, JEOL, Tokyo, Japan) at 80 kV.

Animals

C57BL/6 mice were housed and mated in animal facilities at Chiba University Graduate School of Medicine, with food and acidified water provided ad libitum. Mice were killed by carbon dioxide under NIH guidelines for proper animal procedures, and livers were snap-frozen in liquid nitrogen for storage in −80°C until the experiments.

Indocyanine green uptake study

Indocyanine green (ICG, 25 mg; Dai-ichi Pharm, Tokyo, Japan) was dissolved in 5 ml water in a sterile vial and added to 20 ml each medium at a final concentration of 1 mg/ml. The ICG solution was added to the cell culture and incubated at 37°C for 15 min (Yamada et al. 2002). After the dish was rinsed with PBS, the ICG uptake was observed under microscopy. The number of ICG-positive cells per 100 cells was counted in five different fields. The counting was repeated three times.

Immunostaining

Embryoid bodies were transferred onto 4-chamber glass slides (Clontech, Mountain View, Calif.) coated with gelatin and were fixed with ethanol 18 days after differentiation. Following inactivation of endogenous peroxidase with 2% hydrogen peroxide in methanol, cells were incubated first with 1:500 diluted rabbit anti-mouse albumin antibody (Cappel, Aurora, Ohio) overnight and then with horseradish-peroxidase-labeled anti-rabbit antibody (GE Healthcare Bio-Sciences, Piscataway, N.J.) at a 1:500 dilution. Color was developed with a Dako Envision Kit (DAKO Japan, Tokyo, Japan). Numbers of albumin-positive cells were counted against 100 cells in five different fields by light microsopy, and the ratio of numbers of albumin-positive cells/numbers of counted cells was

calculated. Adult liver (NIH Swiss) fixed in 4% paraformaldehyde and embedded in paraffin was used as positive control (Merck Japan, Tokyo, Japan).

Reverse transcriptase/polymerase chain reaction

Total RNA (5 μg), isolated with Isogen (Nippon Gene, Tokyo, Japan), was used for first-strand cDNA synthesis with Super Script III and oligo (dT) following the manufacturer's instructions (Invitrogen). The polymerase chain reaction (PCR) was performed with *Taq* DNA polymerase (Applied Biosystems Japan, Tokyo, Japan). The PCR primers, annealing temperature, and number of cycles, and the length of the amplified products were as below: Oct3/4 (GenBank accession no. NM_013633, 5′-TCTTT CCACCAGGCCCCCGGCTC, 5′-TGCGGGCGGA CATGGGGAGATCC; 65°C; 30 cycles, 224 bp), Nanog (GenBank accession no. AB093574, 5′-CAGGTGTTT GAGGGTAGCTC, 5′-CGGTTCATCATGGTACAGTC; 50°C; 30 cycles; 223 bp), HNF-3β (GenBank accession no. L10409, 5′-TCAAGTGTGAGAAGCAACTG, 5′-GACGACATGAGGTTGTTGAT; 58°C; 30 cycles; 391 bp), Dlk-1 (GenBank accession no. NM_010052, 5′-ATGCTTCCTGCCTGTGC, 5′-GCACGGGCCACTGGC; 58°C; 30 cycles; 200 bp), transthyretin (TTR; GenBank accession no. BC024701, 5′-CTCACCACAGATGAGAAG, 5′-GGCTGAGTCTCTCAATTC; 55°C; 40 cycles; 225 bp), α-feto protein (AFP; GenBank accession no. BC066206, 5′-TCGTATTCCAACAGGAGG, 5′-AGGCTTTTGCTT CACCAG; 55°C; 40 cycles; 173 bp), albumin (GenBank accession no. BC049971, 5′-GTCTTAGTGAGGTGGAG CAT, 5′-ACTACAGCACTTGGTAACAT; 58°C; 35 cycles; 569 bp), tyrosine aminotransferase (TAT) (GenBank accession no. BC024120, 5′-ACCTTCAATCCCATCCGA, 5′-TCCCGACTGGATAGGTAG; 50°C; 30 cycles; 206 bp), α1-antitrypsin (GenBank accession no. M33567, 5′-CAAT GGCTCTTTGCTCAACA, 5′-AGTGGACCTGGGC TAACCTT; 63°C; 30 cycles; 518 bp), glucose-6-phosphatase (G6P; GenBank accession no. U00445, 5′-CAGG ACTGGTTCATCCTT, 5′-GTTGCTGTAGTAGTCGGT; 55°C; 40 cycles; 210 bp), phosphoenol pyruvate carboxykinase (PEPCK; GenBank accession no. AF009605, 5′-TCTGCCAAGGTCATCCAGG, 5′-GTTTTGGGG ATGGGCACTG; 55°C; 40 cycles; 290 bp), cytokeratin (CK)8 (GenBank accession no. BC094009, 5′-ATCGAGAT CACCACCTACCG, 5′-TGAAGCCAGGGCTAGTGAGT; 55°C; 25 cycles; 127 bp), CK18 (GenBank accession no. BC089022, 5′-CGAGGCACTCAAGGAAGAAC, 5′-CTTGGTGGTGACAACTGTGG; 55°C; 25 cycles; 247 bp), CK19 (GenBank accession no. AB033744, 5′-TGA TCGTCTCGCCTCCTACT, 5′-CAAGGCGTGTTCTGTCT CAA; 55°C; 25 cycles; 262 bp), γ-glutamyl transpeptidase (G-GTP; GenBank accession no. U30509, 5′-AACTTCAT CAAGCCAGGTAAGCAG, 5′-TGACTTCTGTAT GGTGGTGCCG; 58°C; 40 cycles; 289 bp), OTC (GenBank accession no. BC024893, 5′-ACTGTCCACAGAAACA GGC, 5′-ATCCAGCTGAGGGTAAGACC; 55°C; 40 cycles; 300 bp), PAH (GenBank accession no. NW 001843471, 5′-TCGCTATGACCCCTACACTC, 5′-GGTTGACCTCC TAAGTTCTG; 58°C; 40 cycles; 167 bp), GK (GeneBank accession no. U48403, 5′-ATCCGCTGGCTAAGAGA CAACC, 5′-TGCACTGGGCTCCCAATAAGG; 58°C; 40 cycles; 140 bp), galactokinase (GenBank accession no. AF246459, 5′-CATCACCAACTCCAATGTCCG, 5′-ATGCGACTGCCATAAACCCC; 60°C; 40 cycles; 366 bp), and β-actin (GenBank accession no. NM_007393, 5′-TTCCTTCTTGGGTATGGAAT, 5′-GAGCAATGATCTT GATCTTC; 55°C; 40 cycles; 206 bp).

Northern blot analysis

Total RNA (1 μg) was subjected to electrophoresis in a denaturing formaldehyde-agarose gel and transferred to a nylon filter. Hybridization was performed with a DIG Northern starter kit (Roche) following the manufacturer's instructions. A *Pst*I-*Sst*I fragment from 0.35xbC/EBP, kindly provided by Dr. Kleanthis G. Xanthopoulos (Anadys Pharmaceuticals, San Diego, Calif.), was used as a probe for C/EBPα, and a *Bam*HI fragment from pCDANII/mC/EBPβ as a probe for C/EBPβ. Images were scanned and analyzed with ImageJ 1.34 s (National Institutes of Health, Bethesda, Md.). The intensity of 28S rRNA was used as the internal control. The expression levels of C/EBPα and C/EBPβ were calculated as their signal intensity divided by that of 28S rRNA. The experiments were repeated three times.

Statistical analysis

One-factor analysis of variance was performed for statistical analysis with JMP5.0J (SAS Institute Japan, Tokyo, Japan). A P-value of <0.05 was accepted as statistically significant.

Results

Decrease of colony size in HSM

Our initial goal was to enrich cells differentiating to hepatocytes. In ESM, the colonies grew constantly, and the types of cells varied while forming gland-like structures. In HSM, the size of the colonies did not change significantly until day 14. On day 18, unexpectedly, their size dramatically decreased (Fig. 1f). On day 28, most of the cells in HSM had disappeared, as HSM was not suitable

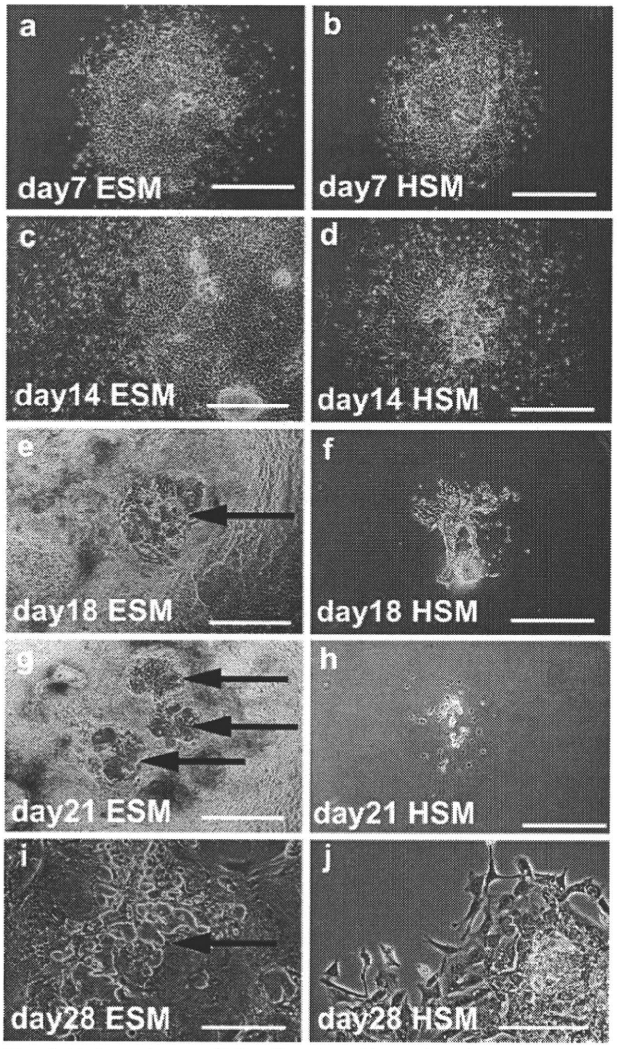

Fig. 1 Embryonic stem (ES) cells cultured in medium lacking leukemia inhibitory factor (*ESM*) versus hepatocyte-selection medium (*HSM*). ES cells were cultured in ESM as embryoid bodies for 4 days, transferred onto dishes coated with gelatin, and then grown in ESM or HSM. **a**, **c**, **e**, **g** Colonies in ESM grew constantly and gland-like structures appeared (*arrows*). **b**, **d**, **f**, **h** Colonies in HSM grew until day 14 but shrank toward day 28. Colonies in ESM consistently contained various types of cells with a gland-like structure (**i**, *arrow*), whereas those in HSM appeared as polygonal cells (**j**). Original magnifications: ×40 (**a–h**), ×200 (**i**, **j**). *Bars* 250 μm (**a–h**), 50 μm (**i**, **j**)

for their survival (Fig. 1h). Colonies in ESM at day 28 contained gland-like structures (Fig. 1i). Cells surviving in HSM beyond day 18 were uniquely polygonal and were firmly attached to each other (Fig. 1j).

Electron-microscopic analysis

Well-grown colonies of hepatocyte-like cells in culture dishes were selected (Fig. 2a); these cells showed cell division (Fig. 2b) and binuclei (Fig. 2b, inset). Electron-microscopic analysis revealed that most of these cells possessed a large nucleus and scanty cytoplasm (Fig. 2c, d). Interestingly, where three or four cells met, the intercellular space was enlarged and contained short microvilli (Fig. 2c,d). The intercellular connection was held intact during cell division (Fig. 2d). Adherens junctions

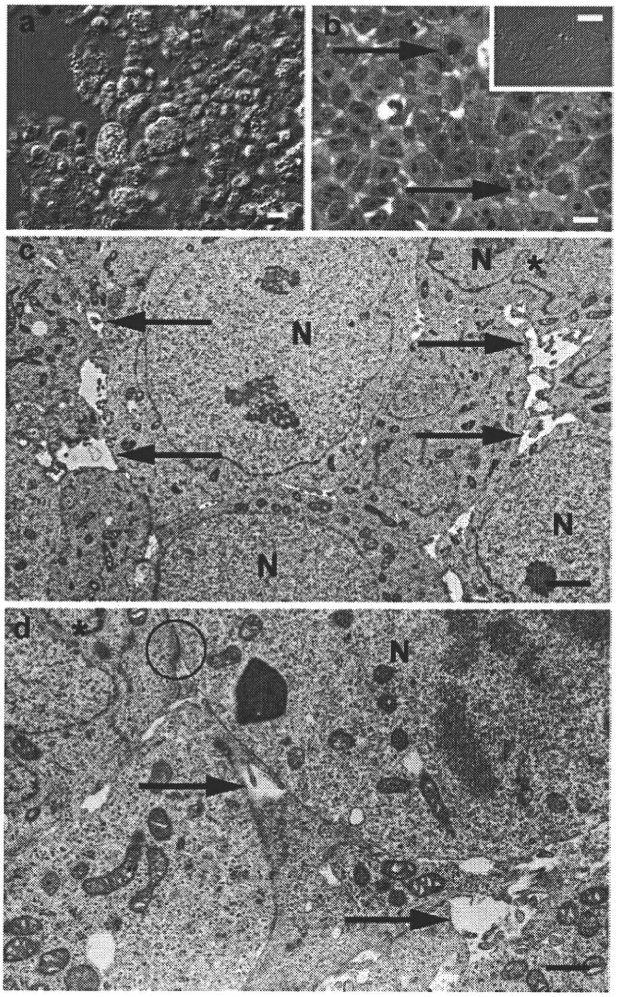

Fig. 2 Light- and electron-microscopic analyses. **a** Differential interference contrast (unfixed) image with Hoechst 33342 staining for live cells (*blue*). **b** Light-microscopic images obtained after toluidine-blue staining (*blue*), corresponding to **a** (*arrows* cells undergoing mitosis). *Inset*: Binucleated cells were sometimes found corresponding to frequent mitosis (*arrows* in **b**). Nuclei were stained with Hoechst 33258. **c**, **d** Electron-microscopic images from a sample similar to the cell mass shown in **a**, **b** (*N* nucleus). Each cell in the colonies possessed a large nucleus and scanty cytoplasm (**c**, **d**). At the point where three or four cells met, the intercellular space was enlarged and contained short microvilli (*arrows* in **c**, **d**). Intercellular connections remained intact during cell division (*circle* in **d**). The nucleus had deep invaginations in many cells (*stars* in **c**, **d**). In higher magnification images (**d** cell division phase), the abundant free ribosomes and a small number of rough endoplasmic reticulum were seen in the cytoplasm. The smooth endoplasmic reticulum was poorly developed. Mitochondria, cytoskeletal components, and Golgi apparatus were well developed. Glycogen was occasionally found. *Bars* 10 μm (**a**, **b**), 5 μm (*inset* in **b**), 1 μm (**c**), 2 μm (**d**)

were found (Fig. 2c), and gap junctions were observed (not shown). Tight junctions were not observed in this study. The nucleus had deep invaginations and prominent nucleoli. The cytoplasm contained abundant free ribosomes and small numbers of rough endoplasmic reticulum. The smooth endoplasmic reticulum was poorly developed. Mitochondria and cytoskeletal components were well developed and at an average level. The Golgi apparatus had also developed normally. Glycogen was not abundantly found in this study.

Cell number

On day 0, 3×10^3 cells were transferred into each well of a 6-well plate (Fig. 3). On day 7 after differentiation, the cell number had increased to $(6.0\pm0.5)\times10^3$ (average±SD) in wells containing ESM, whereas it only showed a slight increase to $(4.1\pm0.4)\times10^3$ in wells with HSM. On day 18, the cell number had increased significantly to $(5.7\pm0.6)\times10^4$ in wells with ESM ($P<0.05$) but had decreased to $(1.1\pm0.2)\times10^3$ in wells with HSM ($P<0.05$). These data clearly showed that only a small number of cells survived in HSM.

ICG uptake and albumin staining

ICG uptake and albumin overexpression are useful hepatocyte markers. ICG was diffusely or granularly detected in the cytoplasm of many cells in HSM (Fig. 4b), whereas only a limited number of cells were ICG-positive in ESM (Fig. 4a): 88±10% of cells in HSM were positive for ICG, but only 1.7±0.2% of cells in ESM were positive for this marker (Fig. 4d). ICG-negative cells were small and polygonal (Fig. 4c). All cells in HSM were strongly positive for albumin in their cytoplasm (100%; Fig. 4h), whereas no cells in ESM were albumin-positive (0%; Fig. 4f). The cytoplasm of hepatocytes of adult liver was positive (Fig. 4j).

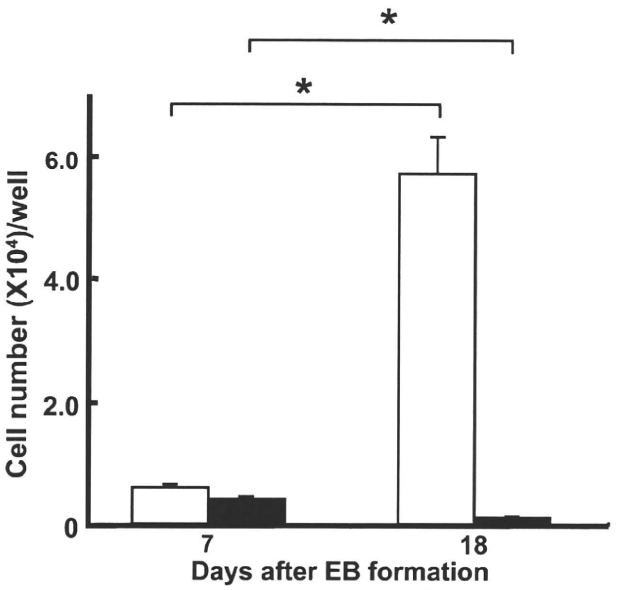

Fig. 3 Cell number in ESM versus HSM: 3×10^3 cells were cultured in each well of 6-well plates coated with gelatin and containing either ESM or HSM. Cell number was counted at 7 and 18 days after formation of embryoid bodies (*EB*). Cell number significantly increased in ESM ($P<0.05$), whereas it apparently decreased in HSM ($P<0.05$). *Open bars* Cell number in ESM, *closed bars* cell number in HSM, *error bar* standard deviation, *$P<0.05$, $n=3$

Expression of liver-specific genes

We characterized cells in ESM or HSM by reverse transcriptase/polymerase chain reaction (RT-PCR) for the expression of genes specific for hepatocytes (Fig. 5a,b). Oct3/4 and Nanog, markers of pluripotent cells, were positive in ES cells, cells grown in ESM, and those cultured in HSM, but negative in fetal and adult liver. HNF-3β, an endodermal marker, was positive in cells in ESM and HSM, fetal liver, and adult liver. Dlk-1, a hepatoblast marker, was positive in cells in ESM and HSM and fetal liver. TTR and AFP were positive in cells in ESM and in HSM. TAT, α1-antitrypsin, G6P, and PEPCK were negative in cells in both ESM and HSM. Interestingly, albumin mRNA was weakly but still distinctly expressed in cells in HSM and at a marginal level in cells in ESM. CKs are markers of epithelial cells; CK8, CK18, and CK19 were positive in cells in both HSM and ESM. CK19 was negative in adult liver. G-GTP was expressed strongly in ES cells and fetal liver and very faintly in cells in HSM. G-GTP was not expressed in cells in ESM or adult liver. OTC and PAH were negative in cells in HSM and ESM. GK was positive in all samples. Galactokinase and PK were positive in cells in HSM, but negative in those in ESM. We also examined the expressions of C/EBPα and C/EBPβ, liver-specific transcription factors involved in hepatoctye differentiation, by Northern blot analysis. No expression of C/EBPα was observed in cells in ESM, but weak expression was seen in cells in HSM (Fig. 5c). With regard to C/EBPβ, weakly positive expression was observed in undifferentiated ES cells (Fig. 5d), and significantly stronger expression was seen in grown cells in HSM than those cultured in ESM, the expression in HSM being at almost the same level as that in fetal liver. Increased expression of C/EBPα and C/EBPβ compared with adult was a feature consistent with previous reports (Nagy et al. 1994).

Discussion

In preliminary experiments, we cultured embryoid bodies in ESM for 4 days, after which we cultured them in ESM for 21 days when hepatocytes are fully differentiated in mouse

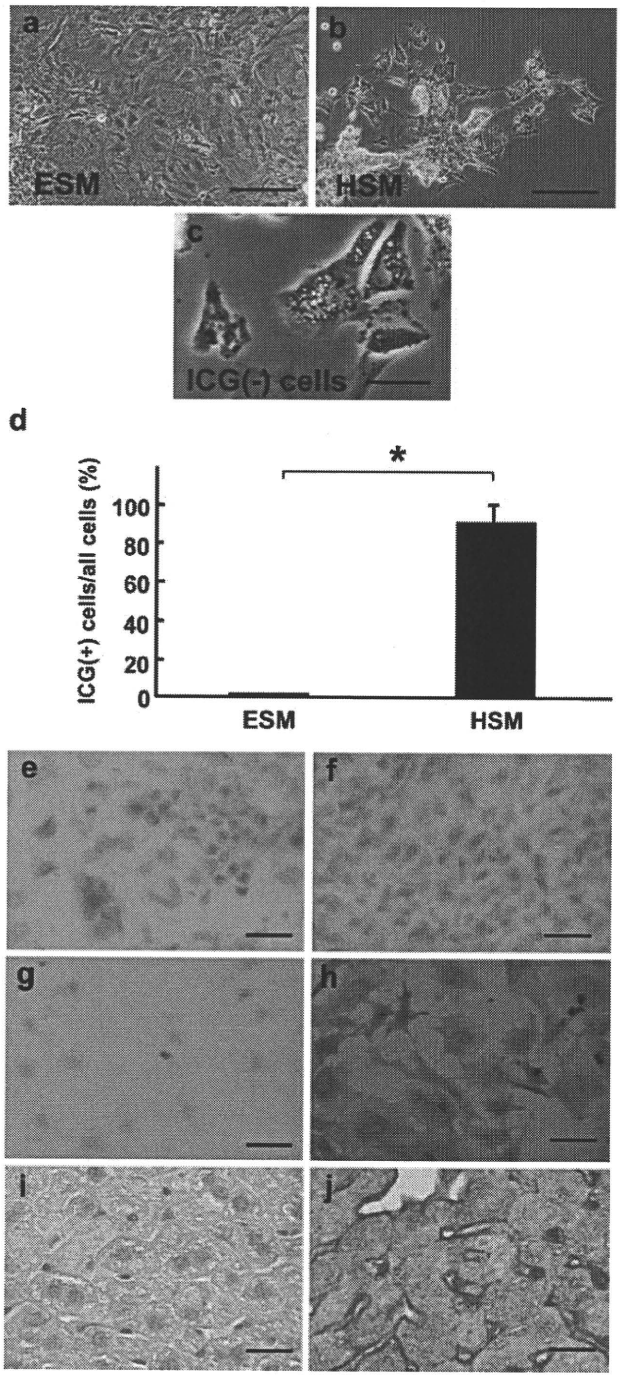

◀ **Fig. 4** ICG uptake and albumin staining. **a–c** At 18 days after the formation of embryoid bodies, 1 mg/ml ICG was added to the medium for 15 min, and the cells were observed microscopically. Most of the cells in HSM (*HSM*) contained fine granules of ICG in their cytoplasm (**b**), but only a small number of cells in ESM (*ESM*) were positive (**a**). ICG-negative cells (*ICG(−)*)were small and polygonal (**c**). **d** Numbers of ICG-positive cells (*ICG(+)*) per 100 cells were counted in five different fields and were significantly higher in HSM than in ESM ($P<0.05$). **e–h** Cells in ESM and HSM were stained with anti-albumin antibody 18 days after the formation of embryoid bodies. The cytoplasm of all cells was strongly positive for albumin in HSM (**h**), but not in ESM (**f**). **j** Positive control: Adult liver was stained with anti-albumin antibody; hepatocytes of adult liver were strongly positive for albumin. **e**, **g**, **i** Negative controls: ES cells in ESM (**e**) or HSM (**g**) 18 days after the formation of embryoid bodies or adult liver (**i**) stained without anti-albumin antibody. Original magnifications: ×50 (**a**, **b**), ×100 (**c**), ×40 (**e–j**). *Bars* 25 μm (**a**, **b**), 5 μm (**c**),

uterus, and then cultured them for 20 days in either ESM or HSM. Three embryoid bodies were spread in wells of 6-well plates (3×10^3 cells). After 20 days of culture in either ESM or HSM with above protocol, each well had 1.3×10^6 cells in ESM but 4.0×10^5 cells in HSM. ICG-positive cells accounted for 1.5% of the cells in ESM but 50% in HSM, suggesting that HSM did not sufficiently enrich cells differentiating to hepatocytes in this protocol. We speculated that cells cultured in ESM for 21 days expressed genes specific to hepatocytes. Day 4 was thus chosen on which to change the medium in order to delete most of the cells, before they acquired the expression of hepatocyte-specific genes. The sizes of the colonies were the same between ESM and HSM until day 14. Suddenly on day 18, the size of the colonies in HSM dramatically decreased. ES cells started to differentiate once LIF was withdrawn, and their function changed constantly. Possibly, they maintained their function to survive HSM with dialyzed serum as nutrition prior to day 14. Beyond day 14, they lost the function, and the surviving cells were those differentiating toward hepatocytes. This hypothesis was supported by the results of RT-PCR. Cells in ESM down-regulated the expression of galactokinase and GK. The disappearing cells were not analyzed because they were degraded and fragmented and were difficult to identify in advance. In the preliminary experiments using 21 days to apply selection, cell numbers decreased, but OTC was negative as revealed by RT-PCR. The percentage of ICG(+) cells was lower. We speculated that (1) on day 4, cells had appeared that were differentiating toward hepatocytes, (2) other cells did not express any of the liver-specific genes. Therefore, we concluded that day 4 was more appropriate for the application of selection pressure. The culture of embryoid bodies in HSM significantly reduced the cell numbers, and 88% of surviving cells were positive for ICG. An enlarged intercellular space and microvilli were observed by electron microscopy. Almost all cells surviving in HSM were positive for albumin. Since ICG uptake and albumin expression are markers of hepatocytes, we concluded that HSM was highly efficient in causing the enrichment of hepatocytes from differentiating ES cells (Teratani et al. 2005; Yamada et al. 2002). Using this method, we did not need to introduce any genes into the ES cells nor manipulate colonies, but simply deprived the medium of ingredients. Our method would thus be safer and more straightforward than previously reported methods, and possible ethical problems could be avoided. We changed ESM to HSM at

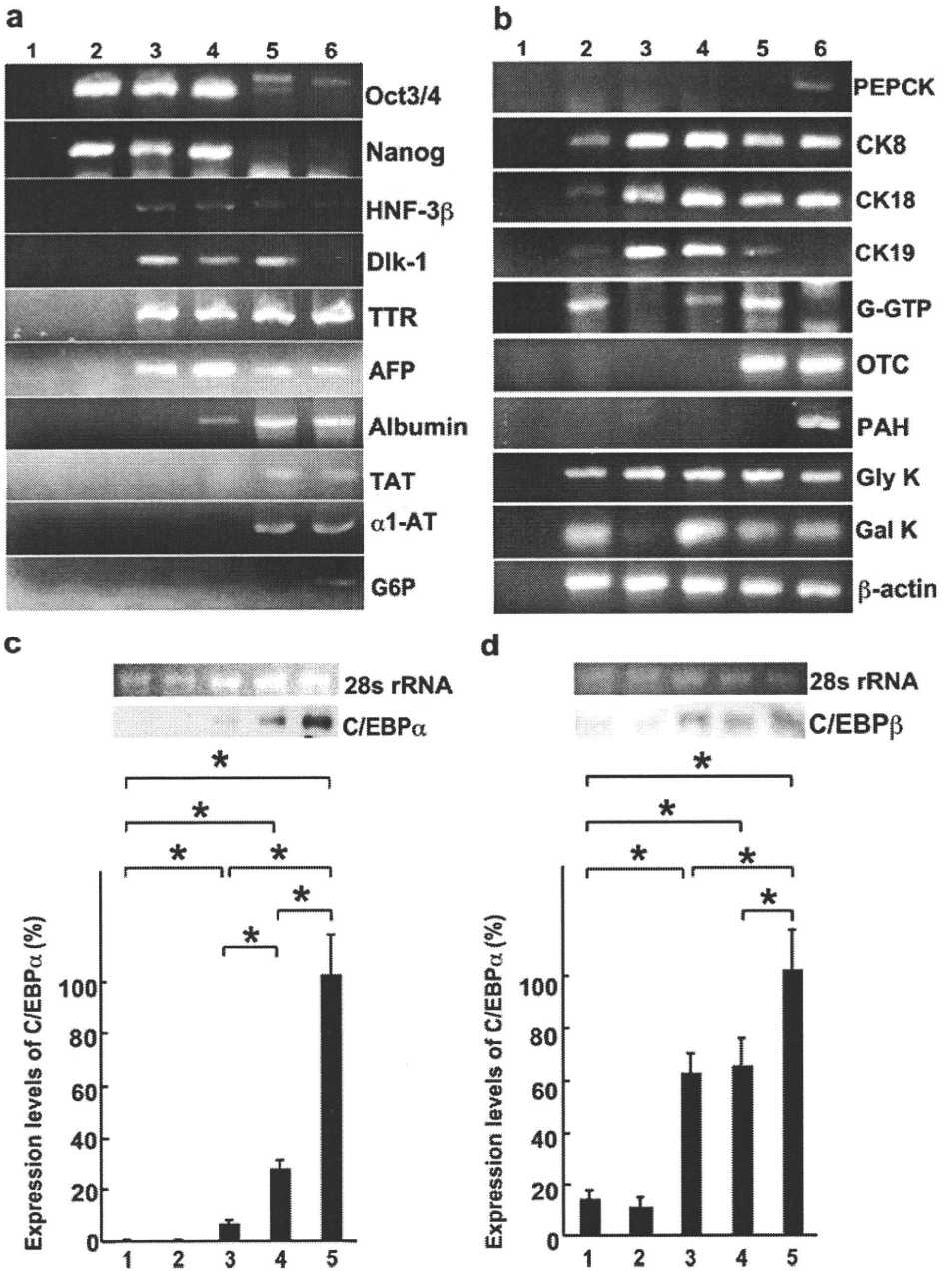

Fig. 5 Expression of liver-specific genes. **a**, **b** RNA was isolated from embryonic stem cells cultured with leukemia inhibitory factor (*lanes 2*), cells cultured in either ESM (*lanes 3*) or HSM (*lanes 4*) 18 days after formation of embryoid bodies, fetal mouse liver at 18.5 days of gestation (*lanes 5*), and adult mouse liver (*lanes 6*). *Lanes 1* Negative control (H_2O). Expression of genes specific for hepatocytes was analyzed with RNA subjected to reverse transcriptase/polymerase chain reaction. Oct3/4, Nanog, HNF-3β, and Dlk-1 were positive in *lanes 3, 4*. *Lane 4* was positive for TTR, AFP, albumin. Interestingly, albumin was not expressed in ESM and only weakly in HSM. CK8, CK18, CK19, and G-GTP were positive in *lane 4*. Note that CK19 and G-GTP were negative in *lane 6*. Galactokinase was positive in *lane 4* but negative in *lane 3* (*TTR* transthyretin, *AFP* α-feto protein, *TAT* tyrosine aminotransferase, *α1-AT* α1-antitrypsin, *G6P* glucose-6-phosphatase, *G-GTP* gamma-glutamyl transpeptidase, *OTC* ornithine transcarbamylase, *PEPCK* phosphoenol pyruvate carboxykinase, *PAH* phenylalanine hydroxylase, *Gly K* glycerol kinase, *Gal K* galactokinase). **c**, **d** C/EBPα and C/EBPβ are hepatocyte-specific transcription factors. Their expression was analyzed by Northern blotting (*lane 1* cells in a medium with LIF, *lane 2* cells in ESM, *lane 3* cells in HSM, *lane 4* fetal mouse liver, *lane 5* adult mouse liver). C/EBPα was not expressed in cells cultured in ESM but was weakly expressed in HSM (**c**). C/EBPβ was expressed in HSM at almost the same level as in fetal liver at 18.5 days of gestation (**d**). The difference between ESM and HSM was significant for C/EBPα (*$P<0.05$, $n=3$; **c**). C/EBPα and C/EBPβ were more strongly expressed in adult liver than in fetal liver at 18.5 days of gestation (*$P<0.05$, $n=3$; **c**, **d**)

the same time as the transfer of embryoid bodies to gelatin-coated dishes and successfully enriched hepatoblast-like cells, whereas cells in ESM remained at a more immature state than those in HSM. We did not use any growth factors specific or extracellular matrix specific to hepatocyte differentiation. We therefore propose that the change of the medium to HSM at 4 days in hanging drop culture is a suitable method for enriching hepatoblast-like cells from ES cells.

Our method with ESM is a spontaneous differentiation protocol (Lavon and Benvenisty 2005). Hanging drop culture for 5 days was used in previous reports, whereas we employed 4 days (Jones et al. 2002; Yamada et al. 2002). Moreover, we used 10% FCS, instead of 15% FCS (Abe et al. 1996), and 14 days of culture of embryoid bodies on gelatin-coated dishes instead of 30 days (Miyashita et al. 2002). Our ESM contained sodium pyruvate, whereas HSM did not, with the apparent promotion of hepatocyte differentiation. Shorter culture in hanging drops, lower levels of FCS, and sodium pyruvate might delay the differentiation of the expression of albumin, although cells in ESM differentiated toward endoderm, as evidenced by the presence of HNF-3β and Dlk-1. The variances in the spontaneous differentiation between our ESM and others might be attributable to a difference in karyotype spectrum, which remains to be determined. We attempted to analyze the karyotype of EB5 but failed because we could not obtain appropriate chromosome spreads in orderly arrangements (Longo et al. 1997).

We next characterized cells surviving in HSM for the expression of genes specific for hepatocytes. Cells should ideally be cultured long-term to allow them to differentiate into more mature or fully differentiated hepatocytes as measured by functional assays, such as urea synthesis. Longer-term culture was however impossible, since cells gradually disappeared beyond 18 days of culture in HSM (Fig. 1f). Expression was therefore analyzed with liver-specific genes. Oct3/4 and Nanog were positive in ESM and HSM but negative in fetal and adult liver. Since Oct3/4 and Nanog are positive in endoderm and in cells more immature than those in fetal liver, cells in ESM and HSM might have differentiated to endodermal cells or hepatoblast-like cells (Jones et al. 2002; Yoshida-Koide et al. 2004). HNF-3β and Dlk-1 were positive in ESM and HSM suggesting that cells in ESM and HSM at least differentiated to a point somewhere between endodermal cells and hepatoblasts. Cells in HSM and ESM were positive for TTR, a visceral endodermal marker, and AFP, an early differentiation marker of hepatocytes (Shiojiri et al. 2004). They were, on the other hand, negative for α1-antitrypsin, G6P, and PEPCK, markers of mature hepatocytes (Hamazaki et al. 2001). Electron microcopy showed that a small number of cells were binuclear, a character of hepatocytes, whereas light microscopy revealed that most of the cells had single nuclei. We speculated that cells in HSM were composed of hepatoblast-like cells in the majority, with mature hepatocytes occurring in small numbers. The RNA of binuclear cells might not have been sufficient to give positive results for α1-antitrypsin, G6P, and PEPCK in RT-PCR. Cells in HSM were obviously more mature than those in ESM, since the former were positive for albumin, whereas the latter were negative, as shown by RT-PCR and immunostaining. Immunoreactivity of albumin progressively increases in parallel with hepatocyte differentiation (Gelly et al. 1991). The albumin expression was stronger in adult liver than cells in HSM as shown by RT-PCR, presumably because the former are more mature than the latter. One possibility was that the cells in HSM or ESM were similar to those of yolk sac or undifferentiated endoderm. Our data clearly showed that they were positive for CK8, CK18, CK19, and G-GTP. Since cytokeratins are markers of epithelial cells, cells in HSM were thought to be differentiated beyond yolk sac or endoderm (Barak et al. 2004). Interestingly, CK19 and G-GTP were negative in adult liver, consistent with previous reports (Ichinose et al. 1989; Ikeda and Taniguchi 2005). On the other hand, CK19 and G-GTP have been reported to be expressed in bile duct epithelial cells (Ichinose et al. 1989; Ikeda and Taniguchi 2005). Since hepatoblasts have the characteristics of both hepatocytes and bile duct epithelial cells, the cells selected in HSM are more likely to have been hepatoblast-like cells (Shiojiri et al. 1991; Shiojiri 1997). Interestingly, electron-microscopic analysis has suggested the formation of bile canaliculi with enlarged intercellular space and microvilli. The expression of C/EBPα and C/EBPβ has been described on 9.5 days of gestation in liver premordium and 15.5 days in liver, respectively (Shiojiri et al. 2004; Nagy et al. 1994). Our Northern blot analysis has shown that C/EBPα is negative in cells in ESM but weakly positive in those in HSM. C/EBPβ is positive in cells in HSM at the same level as that in fetal liver (18.5 days of gestation). Since both genes are deeply involved in the expression of liver-specific genes, these data support our conclusion that HSM successfully "purifies" hepatoblast-like cells.

Unexpectedly, OTC and PAH were not expressed in cells in HSM, which was deprived of arginine and tyrosine in order to select cells expressing these enzymes. This result might be attributable to the production of arginine, as protein degradation and reutilization of amino acid are accelerated without arginine (Bradley 1977). Thus, the withdrawal of arginine and tyrosine is not enough to enrich hepatocytes differentiated from ES cells.

Galactose and glycerol were probably sources of pyruvate for cells in HSM, based on the finding that galactokinase and GK were expressed. Galactokinase was down-regulated when cells differentiated in ESM. The

expression of galactokinase was maintained by the mechanism of cells differentiating toward hepatocytes in HSM. The reason that galactokinase and GK were expressed in ES cells was not clear. One speculation is that these are crucial enzymes deeply involved in energy metabolism and important for the survival of ES cells.

Initially, HSM was expected to enrich hepatocytes differentiating from ES cells. Our data indicated that HSM promoted hepatocyte differentiation. Genes specific for hepatocytes are controlled by hepatocyte-specific transcription factors. To survive HSM, cells need to express hepatocyte-specific enzymes. Hepatocyte-specific transcription factors, therefore, are expressed, promoting hepatocyte differentiatin. This hypothesis is supported by the Northern blot analysis of C/EBPα and C/EBPβ, liver-specific transcription factors. These are more highly expressed in HSM than in ESM.

In the future, we will attempt to develop a method for harvesting large numbers of hepatocyte-like cells, focusing on extracellular matrix and growth factors. In the meanwhile, we recommend the development and refinement of the current method for human ES cells, with the eventual target of transplantation therapy for liver insufficiency.

Acknowledgments The authors thank Dr. Hitoshi Niwa (Center for Developmental Biology, Riken, Kobe, Japan) for providing EB5.

References

Abe K, Niwa H, Iwase K, Takiguchi M, Mori M, Abe SI, Abe K, Yamamura KI (1996) Endoderm-specific gene expression in embryonic stem cells differentiated to embryoid bodies. Exp Cell Res 229:27–34

Ai Y, Jenkins NA, Copeland NG, Gilbert DH, Bergsma DJ, Stambolian D (1995) Mouse galactokinase: isolation, characterization, and location on chromosome 11. Genome Res 5:53–59

Barak V, Goike H, Panaretakis KW, Einarsson R (2004) Clinical utility of cytokeratins as tumor markers. Clin Biochem 37:529–540

Bossard P, Zaret KS (1998) GATA transcription factors as potentiators of gut endoderm differentiation. Development 125:4909–4917

Bradley MO (1977) Regulation of protein degradation in normal and transformed human cells. Effects of growth state, medium composition, and viral transformation. J Biol Chem 252:5310–5315

Gelly JL, Richoux JP, Grignon G, Bouhnik J, Baussant T, Alhenc-Gelas F, Corvol P (1991) Immunocytochemical localization of albumin, transferrin, angiotensinogen and kininogens during the initial stages of the rat liver differentiation. Histochemistry 96:7–12

Hamazaki T, Iiboshi Y, Oka M, Papst PJ, Meacham AM, Zon LI, Terada N (2001) Hepatic maturation in differentiating embryonic stem cells in vitro. FEBS Lett 497:15–19

Heo J, Factor VM, Uren T, Takahama Y, Lee JS, Major M, Feinstone SM, Thorgeirsson SS (2006) Hepatic precursors derived from murine embryonic stem cells contribute to regeneration of injured liver. Hepatology 44:1478–1486

Ichinose Y, Hashido K, Miyamoto H, Nagata T, Nozaki M, Morita T, Matsushiro A (1989) Molecular cloning and characterization of cDNA encoding mouse cytokeratin no. 19. Gene 80:315–323

Ikeda Y, Taniguchi N (2005) Gene expression of gamma-glutamyltranspeptidase. Methods Enzymol 401:408–425

Inoue C, Yamamoto H, Nakamura T, Ichihara A, Okamoto H (1989) Nicotinamide prolongs survival of primary cultured hepatocytes without involving loss of hepatocyte-specific functions. J Biol Chem 264:4747–4750

Ishizaka S, Shiroi A, Kanda S, Yoshikawa M, Tsujinoue H, Kuriyama S, Hasuma T, Nakatani K, Takahashi K (2002) Development of hepatocytes from ES cells after transfection with the HNF-3beta gene. FASEB J 16:1444–1446

Jones EA, Tosh D, Wilson DI, Lindsay S, Forrester LM (2002) Hepatic differentiation of murine embryonic stem cells. Exp Cell Res 272:15–22

Kumashiro Y, Asahina K, Ozeki R, Shimizu-Saito K, Tanaka Y, Kida Y, Inoue K, Kaneko M, Sato T, Teramoto K, Arii S, Teraoka H (2005) Enrichment of hepatocytes differentiated from mouse embryonic stem cells as a transplantable source. Transplantation 79:550–557

Lavon N, Benvenisty N (2005) Study of hepatocyte differentiation using embryonic stem cells. J Cell Biochem 96:1193–1202

Leffert HL, Paul D (1972) Studies on primary cultures of differentiated fetal liver cells. J Cell Biol 52:559–568

Longo L, Bygrave A, Grosveld FG, Pandolfi PP (1997) The chromosome make-up of mouse embryonic stem cells is predictive of somatic and germ cell chimaerism. Transgenic Res 6:321–328

Matsumoto K, Yamada K, Kohmura E, Kinoshita A, Hayakawa T (1994) Role of pyruvate in ischaemia-like conditions on cultured neurons. Neurol Res 16:460–464

McGee MM, Greengard O, Knox WE (1972) The quantitative determination of phenylalanine hydroxylase in rat tissues. Its developmental formation in liver. Biochem J 127:669–674

Miyashita H, Suzuki A, Fukao K, Nakauchi H, Taniguchi H (2002) Evidence for hepatocyte differentiation from embryonic stem cells in vitro. Cell Transplant 11:429–434

Murakami T, Nishiyori A, Takiguchi M, Mori M (1990) Promoter and 11-kilobase upstream enhancer elements responsible for hepatoma cell-specific expression of the rat ornithine transcarbamylase gene. Mol Cell Biol 10:1180–1191

Nagy P, Bisgaard HC, Thorgeirsson SS (1994) Expression of hepatic transcription factors during liver development and oval cell differentiation. J Cell Biol 126:223–233

Nakamura T, Teramoto H, Tomita Y, Ichihara A (1984) L-proline is an essential amino acid for hepatocyte growth in culture. Biochem Biophys Res Commun 122:884–891

Niwa A, Yamamoto K, Sorimachi K, Yasumura Y (1980) Continuous culture of Reuber hepatoma cells in serum-free arginine-, glutamine- and tyrosine-deprived chemically defined medium. In Vitro 16:987–993

Niwa H, Masui S, Chambers I, Smith AG, Miyazaki J (2002) Phenotypic complementation establishes requirements for specific POU domain and generic transactivation function of Oct-3/4 in embryonic stem cells. Mol Cell Biol 22:1526–1536

Ohira RH, Dipple KM, Zhang YH, McCabe ER (2005) Human and murine glycerol kinase: influence of exon 18 alternative splicing on function. Biochem Biophys Res Commun 331:239–246

Phillips JW, Jones ME, Berry MN (2002) Implications of the simultaneous occurrence of hepatic glycolysis from glucose and gluconeogenesis from glycerol. Eur J Biochem 269: 792–797

Shiojiri N (1997) Development and differentiation of bile ducts in the mammalian liver. Microsc Res Tech 39:328–335

Shiojiri N, Lemire JM, Fausto N (1991) Cell lineages and oval cell progenitors in rat liver development. Cancer Res 51:2611–2620

Shiojiri N, Takeshita K, Yamasaki H, Iwata T (2004) Suppression of C/EBP alpha expression in biliary cell differentiation from

hepatoblasts during mouse liver development. J Hepatol 41:790–798

Soto-Gutierrez A, Kobayashi N, Rivas-Carrillo JD, Navarro-Alvarez N, Zhao D, Okitsu T, Noguchi H, Basma H, Tabata Y, Chen Y, Tanaka K, Narushima M, Miki A, Ueda T, Jun HS, Yoon JW, Lebkowski J, Tanaka N, Fox IJ (2006) Reversal of mouse hepatic failure using an implanted liver-assist device containing ES cell-derived hepatocytes. Nat Biotechnol 24:1412–1419

Sumida KD, Crandall SC, Chadha PL, Qureshi T (2002) Hepatic gluconeogenic capacity from various precursors in young versus old rats. Metabolism 51:876–880

Teramoto K, Hara Y, Kumashiro Y, Chinzei R, Tanaka Y, Shimizu-Saito K, Asahina K, Teraoka H, Arii S (2005) Teratoma formation and hepatocyte differentiation in mouse liver transplanted with mouse embryonic stem cell-derived embryoid bodies. Transplant Proc 37:285–286

Teratani T, Yamamoto H, Aoyagi K, Sasaki H, Asari A, Quinn G, Sasaki H, Terada M, Ochiya T (2005) Direct hepatic fate specification from mouse embryonic stem cells. Hepatology 41:836–846

Wheatley DN, Scott L, Lamb J, Smith S (2000) Single amino acid (arginine) restriction: growth and death of cultured HeLa and human diploid fibroblasts. Cell Physiol Biochem 10:37–55

Yamada T, Yoshikawa M, Kanda S, Kato Y, Nakajima Y, Ishizaka S, Tsunoda Y (2002) In vitro differentiation of embryonic stem cells into hepatocyte-like cells identified by cellular uptake of indocyanine green. Stem Cells 20:146–154

Yoshida-Koide U, Matsuda T, Saikawa K, Nakanuma Y, Yokota T, Asashima M, Koide H (2004) Involvement of Ras in extraembryonic endoderm differentiation of embryonic stem cells. Biochem Biophys Res Commun 313:475–481

Zaret KS (2002) Regulatory phases of early liver development: paradigms of organogenesis. Nat Rev Genet 3:499–512

Original Paper

Contrast-enhanced US with Levovist for the Diagnosis of Hepatic Hemangioma: Time-related Changes of Enhancement Appearance and the Hemodynamic Background

Satoshi Kobayashi[1], Hitoshi Maruyama[1], Hidehiro Okugawa[1], Hiroaki Yoshizumi[1] Shoichi Matsutani[2], Masaaki Ebara[1], Osamu Yokosuka[1]

[1]Department of Medicine and Clinical Oncology, Chiba University Graduate School of Medicine and [2]Chiba College of Health Science, Chiba, Japan

Corresponding Author: Hitoshi Maruyama, Department of Medicine and Clinical Oncology Chiba University Graduate School of Medicine, 1-8-1 Inohana, Chuou-ku, Chiba 260-8670, Japan Tel: +81 43 226 2083, Fax: +81 43 226 2088, E-mail: maru@faculty.chiba-u.jp

KEYWORDS: Liver; Hemangioma; Ultrasound; Contrast agent

ABBREVIATIONS: Magnetic Resonance Imaging (MRI); Contrast-Enhanced Computed Tomography (CECT); Ultrasound (US); Contrast-Enhanced US (CEUS); Hepatocellular Carcinoma (HCC); Mechanical Index (MI); Arterioportal Shunt (AP shunt); Microbubble Disappearance Time (MD-T); Nodular Enhancement (NE)

ABSTRACT

Backgrounds/Aims: To elucidate the diagnostic confidence of contrast-enhanced ultrasound (CEUS) with Levovist for hepatic hemangioma.

Methodology: The subjects were 34 patients with 38 hemangiomas and 12 patients with 15 hypervascular hepatocellular carcinomas. The early-phase (15-60 second) and liver-specific phase (after 5 min) were observed by the first injection. The 2nd injection was done for solo-phase method to observe liver-specific phase images without taking early-phase sonograms. The 3rd injection was done for changing posture method to observe liver-specific sonograms under left lateral ducubitus position.

Results: In the early-phase of hemangioma, nodular enhancement (NE) was found transiently in 13 lesions (34%) and continuously in 25 lesions (66%), while hepatocellular carcinoma (HCC, n=15) did not show this pattern. Intratumoral arterioportal shunt was closely related to the short duration of NE. Two enhancement patterns were observed in the liver-specific phase of hemangioma, diffuse in 12 lesions (31%) and partial in 26 lesions (69%), which were dependent on the early-phase enhancement. Liver-specific findings were also affected by taking early-phase sonograms or changing the posture of the patient. This method provided sensitivity of 79% and specificity of 100% for the diagnosis of hemangioma.

Conclusions: CEUS with Levovist may be promising method for the diagnosis of hepatic hemangioma.

INTRODUCTION

Recent advances in digital technologies have resulted in remarkable developments in the field of imaging diagnosis for focal liver lesions (1-4). Although percutaneous needle biopsy has been an essential procedure for the diagnostic standard of liver tumors, there are expectations for their characterization by imaging modalities as a non-invasive method (5-7).

Cavernous hemangioma is the most common tumor among benign focal lesions in the liver (8). Magnetic resonance imaging (MRI) or contrast-enhanced computed tomography (CECT) usually makes the diagnosis, because they have high diagnostic ability based on the characteristic pattern of the tumor (9,10). However, high reliability by ultrasound (US) examination for the diagnosis of hemangioma would be preferable, in terms of the advantages of real-time observation, simple technique and non-invasiveness in clinical practice.

With the development of microbubble contrast agents, contrast-enhanced US (CEUS) has frequently been used for the characterization of liver tumors (1,2,11-15). As for the diagnosis of hemangioma, nodular enhancement (NE) is known as a characteristic enhancement pattern (16-18), and positive enhancement in liver-specific phase is considered to be a characteristic finding of benign liver lesions (14,15). However, some different enhancement patterns have also been reported in CEUS findings of hemangioma (16-18). The variety of the enhancement patterns might be caused by changes of NE during the course of the early-phase enhancement. In addition, static but unstable status of microbubble were supposed to be the causes of different liver-specific patterns, because hemangioma has quite slow blood flow and lacks Kupffer cells which may cause concern about microbubble accumulation in the liver (16-19).

According to this background, CEUS were examined with Levovist both in hepatic hemangioma and HCC, and the time-related changes of contrast-

Hepato-Gastroenterology 2008; 55:1222-1228

enhanced appearances in these 2 tumors were carefully analyzed to present the features of enhancement patterns of hemangioma. Moreover, whether the early-phase observation prior to liver-specific phase or posture of the patient may affect the liver-specific images of hemangioma and HCC was examined to prove the various pattern of liver-specific images of hemangioma. The aim of this study was to elucidate the diagnostic confidence of CEUS with Levovist for hemangioma.

METHODOLOGY

Patients

From July 2005 to January 2007, 34 patients with 38 cavernous hemangiomas in the liver were enrolled in this retrospective study. They consisted of 12 men and 22 women aged from 29-86 years (58±12, mean ± SD). The diagnosis of hemangioma was obtained by CECT in 14 lesions and MRI in 24 lesions, and the size of the lesions ranged from 9.5-137mm (27±22). The number of lesions was one in 31 patients, 2 in 2 patients and 3 in 1 patient and their US pattern were hyperechoic in 22 lesions and hypoechoic in 16 lesions. Thirty patients had normal liver, 3 patients had fatty liver, and 1 patient had liver cirrhosis related to hepatitis C virus.

During the same period, 56 patients with 59 hypervascular HCC lesions underwent CEUS examination before treatment. Among them, additional CEUS examinations to compare their contrast-enhanced findings with hemangioma were done in 12 patients who had enough time for the observation of contrast enhancement under the extra injection of contrast agent. They consisted of 9 men and 3 women aged from 67-83 years (27±10), and all had liver cirrhosis with 15 HCC lesions. Ten patients had hepatitis C virus, but the other 2 patients had neither hepatitis B nor hepatitis C virus. The size of the lesions ranged from 15-52mm (27±10). The diagnosis of HCC was obtained by CECT in 10 lesions and percutaneous needle biopsy in 5 lesions. The depth of the lesions measured between skin surface and its nearest edge of the lesion was 20-100mm (47±22) for hemangioma and 40-100mm (65±25) for HCC.

Therefore, the subjects of this retrospective study were 34 patients with 38 hemangioma and 12 patients with 15 HCCs. Informed consent was obtained by all patients and institutional ethics committee approval was not deemed to be necessary by the chair person for the present study.

Imaging Methods for the Diagnosis of Hemangioma

CECT was performed using Light speed ultra 16 (GE Yokogawa Medical Systems, Hino, Japan). After the injection of 100mL of contrast medium (Iopamiron 300; Nihon Schering, Osaka, Japan) into the antecubital vein at a rate of 3.0mL/s, three-phase images were taken with 5mm collimation (30-s-delay for arterial phase, 80-s-delay for portal phase, and 180-s-delay for equilibrium phase). Imaging criteria for CT images for the diagnosis of hemangioma was a globular peripheral enhancement followed by centripetal fill-in in the arterial phase or a homogenous enhancement in the arterial phase and persistent enhancement during portal phase and were isoattenuating with enhanced intrahepatic vessels (9,20).

MRI was performed using a superconducting system (Signa Horizen; GE Yokogawa Medical Systems, Hino, Japan) operating at 1.5 T. Axial spin-echo (SE) pulse sequences were employed with a *repetition* time (T_R) of 500ms and an echo time (T_E) of 11ms for T_{1W} and T_R of 2000ms and T_E of 80ms for T_{2W}. T1FS were obtained at T_R of 500ms and T_E of 11ms using the chemical shift selective technique to suppress the fat signal. Imaging criteria by MRI for the diagnosis of hemangioma were both low signal intensity on T_1-weighted images and high signal intensity on T_2-weighted images, and high signal intensity on proton-weighted images (10). All the images of CT and MRI were reviewed by M.E., a hepatologist specialized in the reading of CT and MRI images.

US Examination

US examinations were performed with SSA-770A (APLIO, Toshiba, Tokyo, Japan) with a 3.75MHz convex probe. Non-contrast US was performed by tissue harmonic imaging (THI 2.5/5.0), and CEUS was done by wide-band Doppler mode (Advanced Dynamic Flow mode) with intermittent scanning (approximately 1-s intervals). Monitor imaging mode under extra-low mechanical index (MI<0.2) was used to keep the scan plane to support the interval observation. The MI values were between 1.0 and 1.4, and the focal position was set at the bottom of the lesion. The US contrast agent was Levovist (Schering AG, Berlin, Germany), consisting of galactose microparticles (99.9%) and palmitic acid (0.1%). It was administered at a dose of 5.0mL at 300mg/mL (standard dose in Japan) from the antecubital vein as a bolus at a rate of 2.0mL/s followed by a 5mL normal saline flush. After observation with non-contrast US, color Doppler imaging for the lesion was performed to investigate the intratumoral blood flow. When two-parallel vessels showing increased arterial blood flow with reversed blood flow were observed in the lesion on the sonogram, the lesion was diagnosed as hemangioma with intratumoral arterioportal shunt (AP shunt) (21,22). Contrast-enhanced images were taken almost at the median section under breath-holding.

All patient, 34 patients with 38 hemangioma and 12 patients with 15 HCC, received injections of Levovist 3 times, and each injection was done after the disappearance of the prior enhancement. In the present study, the early-phase was defined as the phase 15-60 seconds after the injection and liver-specific phase was defined as the phase contrast enhancement in the portal vein disappeared by the observation of MD-T (23).

US examination was performed by S.K. in 38 patients and by H.Y. in 8 patients, and all sonograms

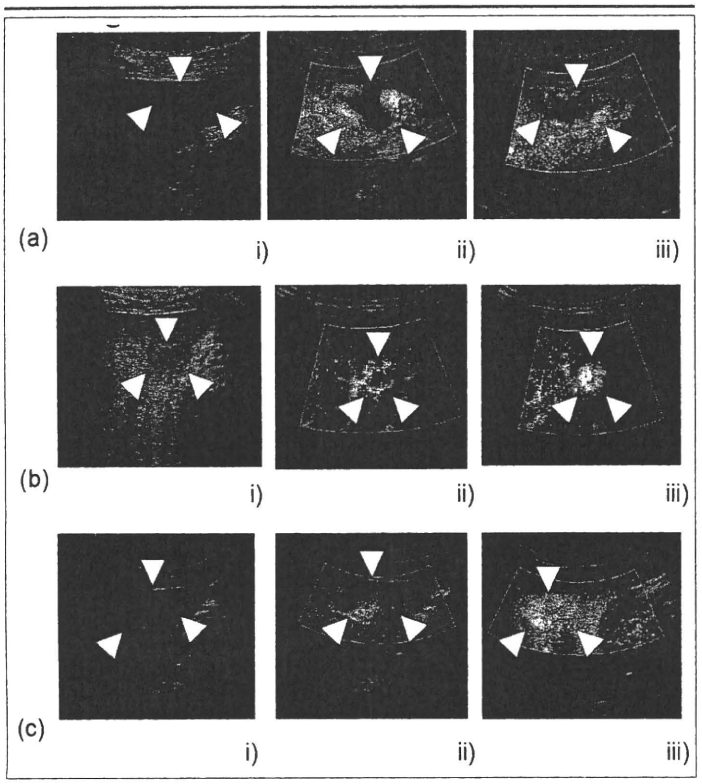

FIGURE 1 Time-related changes of contrast enhancement of hemangioma at the early-phase **(a)** Continuous type. i) Gray-scale. Hyperechoic lesion was seen at segment III in the liver (39mm, arrowheads). ii) Contrast-enhanced sonogram of early-phase (40 s after injection). NE was observed in the lesion. iii) Contrast-enhanced sonogram of early-phase (50 s after injection). NE was observed in the lesion. **(b)** Transient type A. i) Grayscale. Hypoechoic lesion was seen at the segment V in the liver (19mm, arrowheads). ii) Contrast-enhanced sonogram of early-phase (31 s after injection). NE was observed in the lesion. iii) Contrast-enhanced sonogram of early-phase (37 s after injection) The lesion showed whole enhancement following NE, earlier than enhancement of surrounding liver parenchyma. (c) Transient type B. i) Grayscale. Hypoechoic lesion was seen at the segment III in the liver (40mm, arrowheads). ii) Contrast-enhanced sonogram of early-phase (30 s after injection). NE was observed in the lesion. iii) Contrast-enhanced sonogram of early-phase (48 s after injection). The lesion showed whole enhancement following NE, similar to the progression of enhancement in surrounding liver parenchyma.

digitally stored were reviewed by the consensus of H.M. and H.O. The observers and reviewers were hepatologists specialized in US examination.

Standard Method by First Injection

Observation of the early-phase, and subsequent liver-specific phase following the stopping of US transmission to avoid the microbubble breakdown was done under the supine position.

Solo-phase Method by Second Injection

Liver-specific phase images were taken at the time of MD-T without scanning the prior early-phase under the supine position. Contrast-enhanced areas in lesions on liver-specific sonograms were compared quantitatively between the images after taking prior early-phase sonograms and those without taking them, by measurement of the pixel count using Scion Image (Scion Corp., Frederick, MD, USA).

Changing Posture Method by Third Injection

After the observation of the early-phase with the supine position, scanning was stopped and the posture of the patient was changed to the left lateral decubitus position. The same posture was kept until MD-T, and liver-specific sonograms were taken. Liver-specific images by the first injection were compared quantitatively with the images obtained by the changing posture method. The lesion on the sonogram was divided into tetrameric portions by horizontal line and vertical line, and the change of the portions with maximum enhancement between the 2 liver-specific images by 2 methods was considered to be a positive result for the changing posture method.

Statistical Analysis

The Tukey-Kramer test was used to compare the times to continue NE among 3 groups. The chi-square test was used to analyze the relationship between hemangioma and HCC in the solo-phase method and the changing posture method. Stat View version 5 (Abacus Concepts Inc., Berkeley, CA) was employed for the above statistical analysis. The difference with a probability of <5% was considered to be statistically significant ($p<0.05$).

RESULTS

Contrast Enhancement at the Early Phase of Hemangioma

Early-phase sonograms are shown in **Figure 1.** NE was found in all lesions, with 13 lesions showing transiently in the earliest part of the early-phase (transient type, 34%) and 25 lesions showing contin-

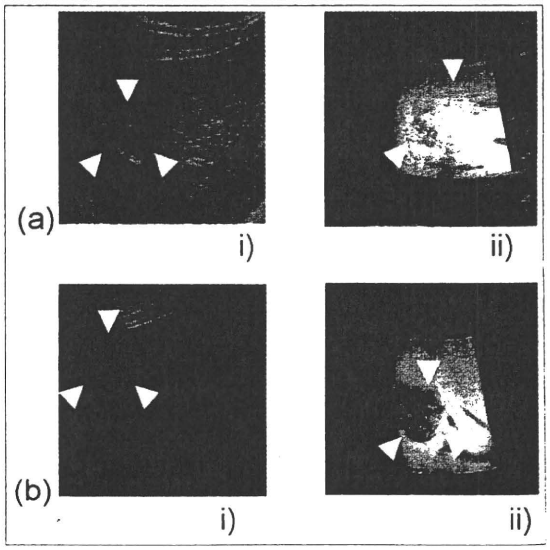

FIGURE 2 Contrast enhancement of hemangioma at liver-specific phase **(a)** Type 1 (diffuse enhancement). i) Grayscale. Hyperechoic lesion was seen at segment VIII in the liver (18mm, arrowheads). ii) Contrast-enhanced sonogram of liver-specific phase. The lesion had diffuse enhancement appearance. (b) Type 2 (partial enhancement). i) Grayscale. Hyperechoic lesion was seen at segment VIII in the liver (36mm, arrowheads). ii) Contrast-enhanced sonogram of liver-specific phase. The lesion had partial enhancement appearance.

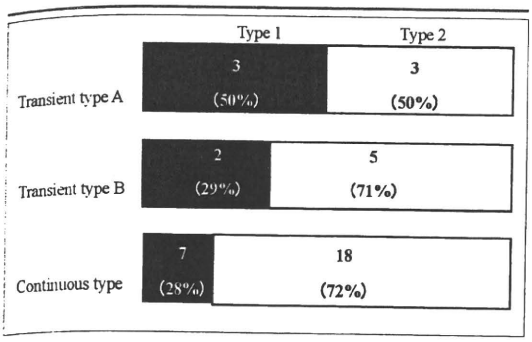

FIGURE 3 Relationship of contrast-enhanced patterns of hemangioma between early-phase and liver-specific phase. Contrast-enhanced findings of liver-specific phase depended on the extent and rapidity of early-phase enhancement in the lesion. Transient type A, B, Continuous type: Early phase. Transient type A: NE was observed transiently in earliest part of early-phase, followed by the whole enhancement of the lesion earlier than surrounding liver parenchyma. Transient type B: NE was observed transiently in earliest part of early-phase, followed by whole enhancement of the lesion similar to the progression of enhancement in surrounding liver parenchyma. Continuous type: NE was observed continuously during early-phase. Type 1, 2: Liver-specific phase. Type 1: Diffuse enhancement. Type 2: Partial enhancement.

uously during the course of the early-phase (continuous type, 66%). Following the transient NE, 6 lesions showed rapid whole enhancement compared to surrounding liver parenchyma (transient type A, 6/13, 46%), and lesions showed gradual whole enhancement almost the same as surrounding liver parenchyma (transient type B, 7/13, 54%). The grade of enhancement in the lesions with continuous type remained a partial enhancement throughout this phase. Color Doppler revealed AP shunt in 4 of the 6 lesions (66%) with transient type A, but in none of the lesions with transient type B and continuous type. The duration time of NE was 4.0±4.2 s (1-11 s) in transient type A, 8.6±4.2 s (4-13 s) in transient type B, and 20±8.7 s (7-37 s) in continuous type, and the duration of continuous type was significantly longer than those of transient types A and B ($p<0.05$). None of the HCC lesions showed NE pattern.

Contrast Enhancement at Liver-specific Phase of Hemangioma

Relationship of contrast enhancement between early-phase and liver-specific phase: Twelve lesions showed diffuse enhancement (Type 1, 31%) and 26 lesions showed partial enhancement (Type 2, 69%) at the liver-specific phase **(Figure 2)**. The extent and rapidity of early-phase enhancement in the lesions correlated well with the contrast-enhanced pattern of the liver-specific phase **(Figure 3)**.

Contrast enhancement findings by solo-phase method and changing posture method between hemangioma and HCC: Changes of enhanced area by the solo-phase method are shown in **Figure 4**. The average ratio of the enhanced areas in the liver-specific images after taking early-phase sonograms to those by the solo-phase method was 56% in hemangioma and 7.1% in HCC; none of the lesions showed a decreased enhanced area by this method. When 50% increase was defined as positive result, the change was significantly frequent ($p=0.0002$) in hepatic hemangioma (22/38, 56%) compared to HCC (1/15, 7%), **(Figure 5a)**.

In hemangioma, a positive result by the changing posture method was found in 7 lesions with Type 2 enhancement at the liver-specific phase of the 38 lesions, **(Figure 5b)**. None of HCC lesions showed positive results by this method. However, the frequency of the changes of contrast-enhanced appearances by this method was not statistically significant between hemangioma and HCC ($p=0.0744$).

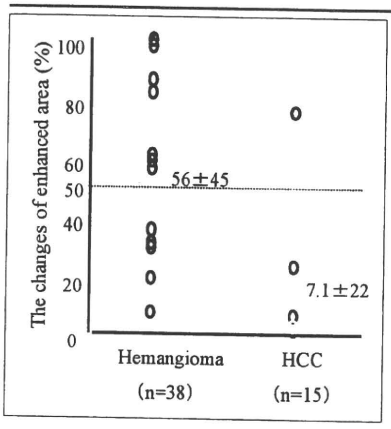

FIGURE 4 Changes of enhanced area by solo-phase method. Averaged ratios of enhanced area on liver-specific images after taking early-phase sonograms to those by solo-phase method were 56% in hemangioma and 7.1% in HCC.

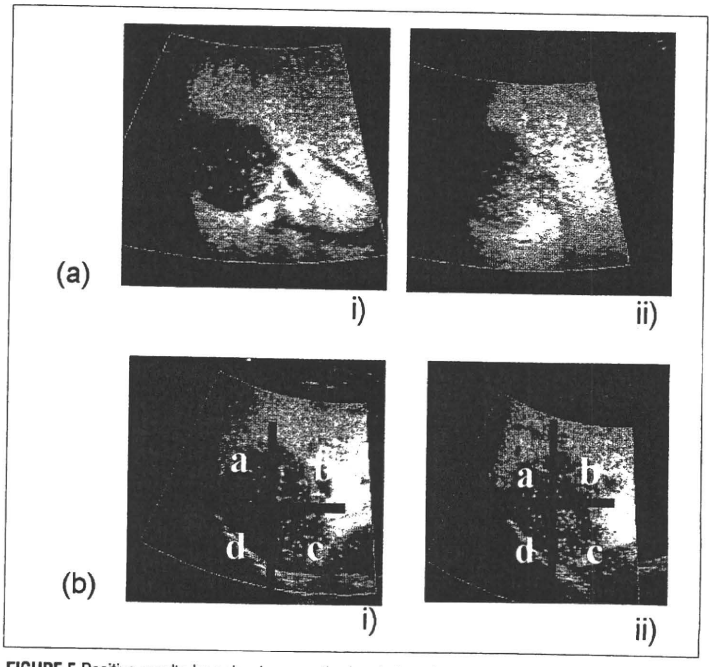

FIGURE 5 Positive results by solo-phase method and changing posture method in hemangioma. **(a)** Solo-phase method. i) Liver-specific image after taking early-phase sonograms. ii) Liver-specific image without taking early-phase sonograms. Enhanced area increased by 100% with solo-phase method. **(b)** Changing posture method. i) Liver-specific image taken in supine position. ii) Liver-specific image taken by changing posture method. The position with maximum enhancement changed from "b" to "c" in this case.

Diagnostic Ability of Hemangioma by CEUS with Levovist

Based on the NE pattern, sensitivity, specificity and accuracy for the diagnosis of hemangioma by CEUS were 100, 100 and 100%, respectively, regardless of the duration of enhancement. However, based on continuous NE, sensitivity, specificity and accuracy were 66, 100, and 66%, respectively. Sensitivity improved by adding the solo-phase method and the changing posture method, from 66 to 79%.

DISCUSSION

Since cavernous hemangioma is the most common disease among benign liver lesions, improvement of the diagnostic ability is important for management of the disease (8). Because of the non-invasiveness and the convenience of the procedure, US examination as a diagnostic tool of focal liver lesions is viewed with high expectations in clinical practice.

All lesions in the present study showed the NE pattern which is well known as a characteristic pattern of hemangioma in the course of contrast enhancement with Levovist (16-18). However, 34% of the lesions showed this pattern transiently and briefly, and only in the earliest part of the early-phase. As the beginning time of contrast enhancement after the injection of contrast agent depends on each patient, observation of this pattern may not always be certain to allow a diagnosis. These results suggest that the definite diagnosis for hemangioma should not depend solely on NE.

The results of this study suggested that several enhancement patterns of the hemangioma at the early-phase may be related to the in-flow rate of the microbubbles into the lesion, and the existence of AP shunt may be one of the important factors. As the influence of hemangioma with AP shunt is not rare (24,25), the characteristic findings should be noted at CEUS examinations for focal liver lesions. There were 4 hemangiomas accompanied by AP shunt in the present study, and 2 of the 4 hemangiomas showed weak or negative enhancement appearance on liver-specific sonograms. As these lesions showed rapid enhancement in the early-phase with very short duration of NE, such lesions may be confusing in their differentiation from hypervascular HCC by CEUS findings. Additionally, a wedge-shaped enhancement of liver parenchyma adjacent to the lesion was not observed in the early-phase sonograms of the 4 hemangiomas with AP shunt. This finding was somewhat different from the early-phase findings of CECT (24,25). Although the reason is not clear, peripheral liver parenchyma might not be enhanced due to the breakdown of microbubbles via AP shunt by US transmission under high acoustic pressure. The contrast-enhanced appearance of hemangioma with AP shunt should be examined under low acoustic power transmission which provides less microbubble breakdown in further studies. In any event, the extent and rapidity of contrast enhancement of hemangioma by CEUS could be related to the hemodynamic features that may depend on the collective size of the constituent vascular spaces of the lesion (26).

Recently, some next-generation US contrast agents have become available in clinical practice (27). Because of different organ-specific properties, although Levovist and Sonazoid (GE healthcare, Amersham, Oslo, Norway) accumulate in the liver, both Sonovue (Bracco, Milan, Italy) and Definity (Bristol-Myers Squibb, North Billerica, MA) pass through the hepatic sinusoid without accumulation in the liver (28-31). Furthermore, contrary to the usage of Levovist, a low acoustic power level (low MI), which has less microbubbles breakdown, has been frequently applied for these new agents (32,33). This low-MI technique allows continuous scanning, which has the advantage of real-time observation compared to intermittent scanning like the present study (32-35). Therefore, the proper imaging technique and diagnostic results for hemangioma may be different from those using Levovist. The strategy and diagnostic ability for hemangiomas should be investigated for each agent in further studies.

Although positive enhancement in the liver-specific phase is considered as a characteristic finding for benign lesions in the liver (13-15), liver-specific images of hemangiomas was not always homogeneous in the present study, and the findings depended on the early-phase appearance in comparison to HCC. The results of this study suggest that the in-flow of microbubbles in the early-phase may provide the liver-specific findings of hemangioma, and this accounts for the variety of contrast-enhanced findings of hemangioma.

In the present study, 2 novel approaches for the observation of liver-specific phase were applied. According to the result by the solo-phase method, the breakdown of microbubbles caused by the prior observation for the early-phase affected the liver-specific findings of hemangioma. In comparison to the result in HCC, this may be caused by a difference in the in-flow rate of microbubbles into the lesions in the early-phase. The result by the changing posture method suggests that microbubbles of the liver-specific phase in some hemangiomas stay in a mobile state. Accumulation of microbubbles by Kupffer cells is considered one of the causes for the phenomenon (36), however, Tung *et al.* reported that hemangioma lacked Kupffer cell distribution in their pathological examination (19). In addition, the pathological results in a previous study revealed that hemangioma has large sinusoidal vascular spaces that show pooling of contrast material in angiography and CECT (37). Therefore, these stagnant hemodynamics may be related to the liver-specific sonograms of hemangioma, and findings by the changing posture method may reflect this hypothesis. Collectively, it seems that these 2 novel approaches utilizing unique characteristics of Levovist could become optional methods for improvement of the diagnostic ability of hemangioma.

There were some limitations to the present study. First, the improvement of the sensitivity from 66 to 79% for the diagnosis of hemangioma, was assessed by the criteria based on the continuous type of NE alone. Calculated on the basis of any duration of NE pattern, all hemangiomas were able to be diagnosed by the pattern. The development of digital analysis for the quantitative judgment of the existence of NE pattern may help the diagnosis of hemangioma in spite of the short duration of this pattern. Next, regarding the solo-phase method and changing posture method, the results of hemangioma were compared with those of HCC alone. Although these 2 tumors are typical in terms of focal liver lesions, the results should be compared with other kinds of liver tumors. Additionally all HCC patients in the present study had liver cirrhosis which may influence the penetration of US beam. This point may account for the difference of contrast-enhanced findings between hemangioma and HCC. And finally, the results were based on 1 series of US examination in each patient. Confirmation of reproducibility for enhancement findings might be needed in further studies.

In conclusion, cavernous hemangioma in the liver showed various pattern of contrast enhancement in CEUS with Levovist, according to the hemodynamic features of the tumor. With understanding of the backgrounds, CEUS with Levovist may become an essential tool for the diagnosis of hemangioma in the liver.

REFERENCES

1 **Burns PN, Wilson SR, Simpson DH:** Pulse inversion imaging of liver blood flow: improved method for characterizing focal masses with microbubble contrast. Invest Radiol 2000; 35:58-71.

2 **Maruyama H, Ebara M:** Recent applications of ultrasound: diagnosis and treatment of hepatocellular carcinoma. Int J Clin Oncol 2006; 11:258-267.

3 **Spielmann AL:** Liver imaging with MDCT and high concentration contrast media. Eur J Radiol 2003; 45:S50-S52.

4 **Elsayes KM, Narra VR, Yin Y, et al:** Focal hepatic lesions: diagnostic value of enhancement pattern approach with contrast-enhanced 3D gradient-echo MR imaging. Radiographics 2005; 25:1299-1320.

5 **Nosher JL, Plafker J:** Fine needle aspiration of the liver with ultrasound guidance. Radiology 1980; 136:177-180.

6 **Leen E, Ceccotti P, Kalogeropoulou C, et al:** Prospective multicenter trial evaluating a novel method of characterizing focal liver lesions using contrast-enhanced sonography. AJR Am J Roentgenol 2006; 186:1551-1559.

7 **Kim YK, Kim CS, Chung GH, et al:** Comparison of Gadobenate Dimeglumine-enhanced dynamic MRI and 16-MDCT for the detection of hepatocellular carcinoma. AJR Am J Roentgenol 2006; 186:149-157.

8 **Mergo PJ, Ros PR:** Benign lesions of the liver. Radiol Clin North Am 1998; 36:319-331.

9 **Quinn SF, Benjamin GG:** Hepatic cavernous hemangiomas: simple diagnostic sign with dynamic bolus CT. Radiology 1992; 182:545-548.

10 **Semelka RC, Brown ED, Ascher SM, et al:** Hepatic hemangiomas: a multi-institutional study of appearance on T2-weighted and serial gadolinium-enhanced gradient-echo MR images. Radiology 1994; 192:401-406.

11 **Kim TK, Choi BI, Han JK, et al:** Hepatic tumors: contrast agent-enhancement patterns with pulse-inversion harmonic US. Radiology 2000; 216:411-417.

12 **Isozaki T, Numata K, Kiba T, et al:** Differential diagnosis of hepatic tumors by using contrast enhancement patterns at US. Radiology 2003; 299:798-805.

13 **von Herbay A, Vogt C, Haussinger D:** Late-phase pulse-inversion sonography using the contrast agent Levovist: differentiation between benign and malignant focal lesions of the liver. AJR Am J Roentgenol 2002; 179:1273-1279.

14 **Blomley MJ, Sidhu PS, Cosgrove DO, et al:** Do different types of liver lesions differ in their uptake of the microbubble contrast agent SH U 508A in the late liver phase? Early experience. Radiology 2001; 220:661-667.

15 **Bryant TH, BlomLey MJ, Albrecht T, et al:** Improved characterization of liver lesions with liver-phase uptake of liver-specific microbubbles: prospective multicenter study. Radiology 2004; 232:799-809.

16 **Quaia E, Bertolotto M, Dalla Palma L:** Characterization of liver hemangiomas with pulse inversion harmonic imag ing. Eur Radiol 2002; 12:537-544.

17 **Quaia E, Bartolotta TV, Midiri M, et al:** Analysis of different contrast enhancement patterns after microbubble-based contrast agent injection in liver hemangiomas with atypical appearance on baseline scan. Abdom Imaging 2006; 31:59-64.

18 **Bartolotta TV, Midiri M, Quaia E, et al:** Liver haemangiomas undetermined at grey-scale ultrasound: contrast-enhancement patterns with Sonovue and pulse-inversion US. Eur Radiol 2005; 15:685-693.

19 **Tung GA, Cronan JJ:** Percutaneous needle biopsy of hepatic cavernous hemangioma. J Clin Gastroenterol 1993; 16:117-122.

20 **Kim KW, Kim TK, Han JK, et al:** Hepatic hemangiomas with arterioportal shunt: findings at two-phase CT. Radiology 2001; 219:707-711.

21 **Lin ZY, Chang WY, Wang LY, et al:** Clinical utility of pulsed Doppler in the detection of arterioportal shunting in patients with hepatocellular carcinoma. J Ultrasound Med 1992; 11:269-273.

22 **Naganuma H, Ishida H, Konno K, et al:** Hepatic hemangioma with arterioportal shunts. Abdom Imaging 1999; 24:42-46.

23 **Maruyama H, Matsutani S, Okugawa H, et al:** Microbubble disappearance-time is the appropriate timing for liver-specific imaging after injection of Levovist. Ultrasound Med Biol 2006; 32:1809-1815.

24 **Kim KW, Kim AY, Kim, et al:** Hepatic hemangiomas with arterioportal shunt: sonographic appearances with CT and MRI correlation. AJR Am J Roentgenol 2006; 187:W406-W414.

25 **Byun JH, Kim TK, Lee CW, et al:** Arterioportal shunt: prevalence in small hemangiomas versus that in hepatocellular carcinomas 3cm or smaller at two-phase helical CT. Radiology 2004; 232:354-360.

26 **Yamashita Y, Ogata I, Urata J, et al:** Cavernous hemangioma of the liver: pathologic correlation with dynamic CT findings. Radiology 1997; 203:121-125.

27 **Barr R:** Seeking consensus: contrast ultrasound in radiology. Eur J Radiol 2002; 41:207-216

28 **Maruyama H, Matsutani S, Saisho H, et al:** Different behaviors of microbubbles in the liver: time-related quantitative analysis of two ultrasound contrast agents, Levovist® and Definfity®. Ultrasound Med Biol 2004; 30:1035-1040.

29 **Forsberg F, Liu JB, Merton DA, et al:** Gray scale second harmonic imaging of acoustic emission signals improves detection of liver tumors in rabbits. J Ultrasound Med 2000; 19:557-563.

30 **Forsberg F, Piccoli CW, Liu JB, et al:** Hepatic tumor detection: MR imaging and conventional US versus pulse-inversion harmonic US of NC100100 during its reticuloendothelial system-specific phase. Radiology 2002; 222:824-829.

31 **Lim AK, Patel N, Eckersley RJ, et al:** Evidence for

spleen-specific uptake of a microbubble contrast agent: a quantitative study in healthy volunteers. Radiology 2004; 231:785-788.

32 **Maruyama H, Matsutani S, Saisho H, et al:** Extra-low acoustic power harmonic images of the liver with perflutren: novel imaging for real-time observation of liver perfusion. J Ultrasound Med 2003; 22:931-938.

33 **Wilson SR, Burns PN:** Liver mass evaluation with ultrasound: the impact of microbubble contrast agents and pulse inversion imaging. Semin Liver Dis 2001; 21:147-159.

34 **Ricci P, Laghi A, Cantisani V, et al:** Contrast-enhanced sonography with SonoVue: enhancement patterns of benign focal liver lesions and correlation with dynamic Gadobenate Dimeglumine-enhanced MRI. AJR Am J Roentgenol 2005; 184:821-827.

35 **Fan ZH, Chen MH, Dai Y, et al:** Evaluation of primary malignancies of the liver using contrast-enhanced sonography: correlation with pathology. AJR Am J Roentgenol 2006; 186:1512-1519.

36 **Iijima H, Moriyasu F, Miyahara T, et al:** Ultrasound contrast agent, Levovist microbubbles are phagocytosed by Kupffer cells-In vitro and in vivo studies. Hepatol Res 2006; 35:235-237.

37 **Freeny PC, Vimont TR, Barnett DC:** Cavernous hemangioma of the liver ultrasonography, arteriography, and computed tomography. Radiology 1979; 132:143-148.

Down-Regulation of Hedgehog-Interacting Protein through Genetic and Epigenetic Alterations in Human Hepatocellular Carcinoma

Motohisa Tada,[1,3] Fumihiko Kanai,[1,2] Yasuo Tanaka,[1,2] Keisuke Tateishi,[1] Miki Ohta,[1] Yoshinari Asaoka,[1] Motoko Seto,[1] Ryosuke Muroyama,[1] Kenichi Fukai,[3] Fumio Imazeki,[3] Takao Kawabe,[1] Osamu Yokosuka,[3] and Masao Omata[1]

Abstract

Purpose: Hedgehog (Hh) signaling is activated in several cancers. However, the mechanisms of Hh signaling activation in hepatocellular carcinoma (HCC) have not been fully elucidated. We analyzed the involvement of Hh-interacting protein (*HHIP*) gene, a negative regulator of Hh signaling, in HCC.

Experimental Design: Glioma-associated oncogene homologue (Gli) reporter assay, 3-(4,5-dimethylthiazol-2-yl)-5-(3-carboxymethoxyphenyl)-2-(4-sulfophenyl)-2H-tetrazolium assay, and quantitative real-time reverse transcription–PCR for the target genes of the Hh signals were performed in *HHIP* stably expressing hepatoma cells. Quantitative real-time PCR for *HHIP* was performed in hepatoma cells and 36 HCC tissues. The methylation status of hepatoma cells and HCC tissues was also analyzed by sodium bisulfite sequencing, demethylation assay, and quantitative real-time methylation-specific PCR. Loss of heterozygosity (LOH) analysis was also performed in HCC tissues.

Results: *HHIP* overexpression induced significant reductions of Gli reporter activity, cell viability, and transcription of the target genes of the Hh signals. *HHIP* was hypermethylated and transcriptionally down-regulated in a subset of hepatoma cells. Treatment with a demethylating agent led to the *HHIP* DNA demethylation and restoration of *HHIP* transcription. *HHIP* transcription was also down-regulated in the majority of HCC tissues, and more than half of HCC tissues exhibited *HHIP* hypermethylation. The *HHIP* transcription level in *HHIP*-methylated HCC tissues was significantly lower than in *HHIP*-unmethylated HCC tissues. More than 30% of HCC tissues showed LOH at the *HHIP* locus.

Conclusions: The down-regulation of *HHIP* transcription is due to DNA hypermethylation and/or LOH, and Hh signal activation through the inactivation of *HHIP* may be implicated in the pathogenesis of human HCC.

Hepatocellular carcinoma (HCC) is one of the most common cancers in Asia and Africa, and its incidence is increasing worldwide (1). Despite recent advances in early diagnosis and treatment, the prognosis for HCC remains very poor. Most HCC cases arise in the setting of chronic hepatitis virus infection. Alcohol consumption, dietary aflatoxin, and exposure to chemical carcinogens are also implicated in its pathogenesis (1, 2). Although the etiologic factors involved in HCC are well known, the genetic events underlying its carcinogenesis are still unclear.

The Hedgehog (Hh) pathway is indispensable for human development and tissue polarity (3). The binding of secreted Sonic Hh (*SHH*) and Indian Hh to their receptor, patched (*PTCH*), which represses the activity of the transmembrane protein smoothened (*SMO*) in the absence of ligand, leads to alleviation of *PTCH*-mediated suppression of *SMO* (4). Derepression of *SMO* results in the activation of downstream targets through the activation of the transcription factor, glioma-associated oncogene homologue (*GLI*; ref. 4). Two types of aberrant activation of Hh signaling are involved in carcinogenesis: ligand-independent and ligand-dependent activation. The former is due to oncogenic mutation in signal components, such as *SMO* and *PTCH*, and has been reported in sporadic basal cell carcinoma, medulloblastoma, and Gorlin syndrome, which is characterized by numerous basal cell carcinoma, rhabdomyosarcoma, and medulloblastoma (5–9). Ligand-dependent activation with Hh overexpression has been reported in gastric, pancreatic, prostate, and small cell lung cancers (10–14).

Recently, the aberrant activation of Hh signaling in HCC has also been reported (15–17). The authors showed that the overexpression of *SMO* or induced expression of *SHH* was the

Authors' Affiliations: Departments of [1]Gastroenterology and [2]Clinical Drug Evaluation, Graduate School of Medicine, University of Tokyo, Tokyo, Japan and [3]Department of Medicine and Clinical Oncology, Graduate School of Medicine, Chiba University, Chiba, Japan

Received 5/15/07; revised 10/13/07; accepted 11/30/07.

The costs of publication of this article were defrayed in part by the payment of page charges. This article must therefore be hereby marked *advertisement* in accordance with 18 U.S.C. Section 1734 solely to indicate this fact.

Note: Supplementary data for this article are available at Clinical Cancer Research Online (http://clincancerres.aacrjournals.org/).

Requests for reprints: Fumihiko Kanai, Department of Clinical Drug Evaluation, Graduate School of Medicine, University of Tokyo, 7-3-1 Hongo, Bunkyo-ku, Tokyo 113-8655, Japan. Phone: 81-3-3815-5411, ext. 37025; Fax: 81-3-3814-0021; E-mail: kanaif-int@h.u-tokyo.ac.jp.

doi:10.1158/1078-0432.CCR-07-1181

major trigger for Hh signal activation (16, 17). However, the implication of a negative regulator of Hh signaling was not fully investigated. On the other hand, Hh signaling regulates angiogenesis, and Hh-interacting protein (*HHIP*), which functions as a negative regulator of the Hh pathway (18), is down-regulated in endothelial cells during tube formation (19), suggesting that disruption of the *HHIP* gene may induce vascular-rich tumors, such as HCC. This led us to focus on *HHIP*. The *HHIP* gene is expressed in most human fetal and adult tissues (20) and encodes a membrane glycoprotein that binds all three mammalian Hh proteins, i.e., *SHH*, Indian Hh, and Desert Hh, with affinity similar to that of *PTCH* (21). In the current study, we investigated the involvement of *HHIP* in hepatoma cell lines and the methylation status, loss of heterozygosity (LOH), and mRNA expression of *HHIP* gene in 36 HCC cases.

Materials and Methods

Cell culture. The human hepatoma and hepatoblastoma cell lines HLE, HuH7, HepG2, HuH6, and PLC/PRF/5 were obtained from the Health Science Resources Bank, and Hep3B was obtained from the Cell Resource Center for Biomedical Research. The cell lines were grown in DMEM supplemented with 10% fetal bovine serum, 100 units/mL penicillin, and 100 μg/mL streptomycin.

Patients. Liver tissues were obtained from 36 HCC patients (31 men and 5 women; mean age, 62.3 ± 11.0 y) who underwent surgical resection at Chiba University Hospital. Among these patients, six were positive for hepatitis B surface antigen and 25 were positive for hepatitis C virus antibody, whereas the remaining five patients lacked evidence of either viral infection. Based on the histologic findings, the 36 HCC tumors were classified as follows: 6 well-differentiated, 25 moderately differentiated, and 5 poorly differentiated tumors. More than 50% of the tumors developed in cirrhotic livers (Supplementary Table S1). HCC samples and corresponding nontumor liver tissues obtained by surgical resection were immediately frozen at -80°C. All patients gave informed consent for their participation, and the ethics committee approved these studies.

Establishment of cells with stable expression of **HHIP.** We purchased the full-length human *HHIP* clone that encodes the open reading frame of *HHIP* from GeneCopoeia and inserted it into the pCMV-Tag4 mammalian expression vector (Stratagene), thereby generating the pCMV-Tag4-*HHIP* vector. After confirming the insertion by sequencing, we transfected the pCMV-Tag4-*HHIP* vector or the empty vector (pCMV-Tag4) using Fugene 6 (Roche) into HuH7 and Hep3B cells, which were confirmed as *HHIP*-null cells by quantitative real-time reverse transcription–PCR (RT-PCR) and Western blotting (Fig. 1; data not shown). To establish cell lines that stably express *HHIP*, we cultured the transfected cells in the presence of 800 μg Geneticin (Wako). Geneticin-resistant colonies appeared within 2 wk, after which the cells were expanded for another 3 wk to produce the original stock cells. Four *HHIP* stable transfectants (H7-HHIP1, H7-HHIP2 and 3B-HHIP1, 3B-HHIP2) and two control transfectants (H7-MOCK and 3B-MOCK) were selected for further study.

Western blotting. Western blotting was done using proteins of total fractions and the primary antibodies for rabbit anti-SHH (1:250; Santa Cruz Biotechnology), rabbit anti-*GLI1* (1:1,000; Cell Signaling Technology), rabbit anti-Hip (R&D Systems), mouse anti–β-actin (*ACTB*; 1:10,000; Sigma-Aldrich), and mouse anti-FLAG M2 (1:1,000; Sigma-Aldrich). The appropriate horseradish peroxidase–conjugated antibodies (1:1,000; Amersham) were used as secondary antibodies. An enhanced chemiluminescence detection system (ECL-plus, Amersham) was used for detection. Experimental procedures were performed as previously described (10).

Gli reporter assay. Hepatoma and hepatoblastoma cells lines, *HHIP* stably transfected cells and the control MOCK cells, were seeded into 12-well plates and grown to ~50% to 70% confluence for 24 h before being transiently transfected with 0.5 μg of 8× 3′Gli-BS-δ51 Luc II, a gift from Dr. Hiroshi Sasaki (Center for Developmental Biology, RIKEN; ref. 22) and 50 ng of pRL-SV40 vector (Toyo Ink) using Fugene 6. This Gli-luciferase reporter construct contains eight copies of the consensus Gli-binding site upstream of a δ-crystallin basal promoter (22, 23). Cells were harvested 48 h after transfection, and luciferase assays were performed with the Picagene Dual Sea Pansy system (Toyo Ink). Firefly and sea pansy luciferase activities were measured as relative light units using a luminometer (Lumat LB 9507, EG&G Berthold). All assays were performed at least in triplicate.

Cyclopamine treatment. All six hepatoma and hepatoblastoma cell lines were seeded into six-well plates and grown in medium containing the pharmacologic Hh inhibitors, cyclopamine (Toronto Research Chemicals) at concentrations of 0 to 10 μmol/L for 96 h. We changed the medium every 2 d.

3-(4,5-Dimethylthiazol-2-yl)-5-(3-carboxymethoxyphenyl)-2-(4-sulfophenyl)-2H-tetrazolium assay. The numbers of viable cells were determined using a CellTiter 96 AQ_{ueous} One Solution Cell Proliferation Assay (Promega) according to the manufacturer's instructions. In brief, cells were plated on six-well tissue culture plates at a density of 3.0×10^4 per well. Ninety-six hours after seeding, the cells were incubated with 3-(4,5-dimethylthiazol-2-yl)-5-(3-carboxymethoxyphenyl)-2-(4-sulfophenyl)-2H-tetrazolium (MTS) reagent solution for 2 h at 37°C. The absorbance at 490 nm was recorded using an ELISA plate reader. All assays were performed at least in triplicate.

5-Aza-2′-deoxycitidine treatment. For demethylation experiments, all six hepatoma and hepatoblastoma cells were plated at a density of 5.0×10^5 cells/100-mm dish and cultured for 24 h, followed by 96 h of culturing with 1 μmol/L 5-aza-2′-deoxycitidine (5-aza-CdR; Sigma-Aldrich).

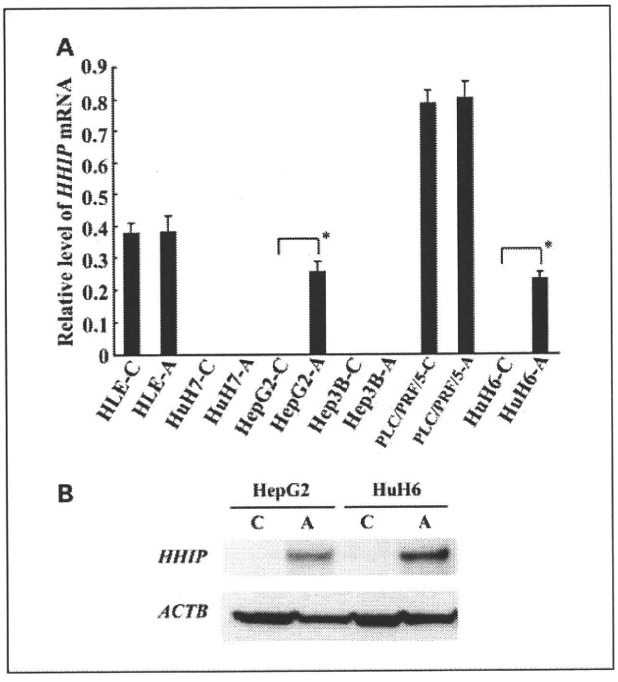

Fig. 1. *A*, relative levels of *HHIP* mRNA expression in hepatoma and hepatoblastoma cell lines. Columns, mean from the results of three independent experiments; bars, SD. *, $P < 0.0001$. *B*, *HHIP* protein expression in HepG2 and HuH6 cells with or without 5-aza-CdR treatment: *C*, control (without 5-aza-CdR treatment); *A*, treated with 5-aza-CdR.